



An early indicator index of tornadic storms for Euro-Mediterranean region

Omer Kutay Mihliardic¹ · Sevinc Asilhan Sirdas² · Serkan Kaya³

Received: 16 March 2023 / Accepted: 29 October 2023
© The Author(s) 2023

Abstract

Tornadoes are the most violent and destructive of all the severe weather phenomena that localized convective storms produce. There is a requirement in operational meteorology increasing nowadays that an indicator index which allows to reduce the uncertainty of severe convective storms and tornadoes in the scope of climate change adaptation strategies. The main intention is not to replace or substitute mesoscale modeling approaches, or composite indexes, but to warn operationally to draw attention to the Eastern Mediterranean and Türkiye in particular a few days in advance. The development of some indicators using atmospheric variables can undertake a crucial role by enabling such numerical models to be run only at certain time intervals, thus enduring lower computational costs. In this study, Eastern Mediterranean oscillation index (EMEDO_i) has been developed in order to be able to detect the presence of ULLs (upper-level low) and frontogenesis approach is employed for selected tornadic storm events in Türkiye. EMEDO_i has 7 different its variations (members) which these members have been developed to detect differences depending on the entry directions of cyclones and storms influencing Türkiye from the west of the country. In line with the GDAS data analysis, values of geopotential height are derived for the requirement of EMEDO_i in a limited area. A few of the results from the study are as in the following: 86% of the trained tornado events revealed that the EMEDO-Oper index was in negative phase at the time a tornado was reported, regardless of whether the events featured a supercell mesoscale convective storm or a frontal movement. The hourly period until the local minimum is obtained can be described and characterized as the process by which the EMEDO-Oper index value decreases continuously. The time required to reach the local minimum varies based on the tornado occurrence. Based on the tornadic storm scenario in the test cluster in 2022 and the train cluster, this timeframe is predicted to be roughly 33.2 h on average. In western Türkiye, there is a 79% chance of a tornado occurring between six and forty-two hours after the EMEDO-Oper index reaches its local minimum. In particular, the projected chance for this period is 63% between 12 and 30 h after the local minimum is obtained. Besides, the majority of the tornado incidents with EMEDO-Oper values below -0.75 were evaluated. After an EMEDO-Oper index value falls below that threshold, it is likely to forecast the risk period of a tornado in Türkiye with a probability of 79% and the local minimum point must be identified.

Extended author information available on the last page of the article

Keywords Tornado · Eastern Mediterranean oscillation index (EMEDO_i) · Extreme weather events · Low-level jet · Severe convective storm

1 Introduction

Severe convective storms worldwide inflict damage to property and crops, disrupt air, sea, and ground travel and outdoor activity, and, in the most extreme cases, inflict injuries and even death. In terms of defining a convective storm as severe/non-violent, measurable or calculable parameters associated with important weather events, which often exceed certain local threshold values (Doswell 2001). Regardless of whether or not there is actual damage; the Storm Prediction Center (SPC) of the National Weather Service (NWS) in the U.S. describes “severe” weather associated with local storms (as opposed to storms that are much larger in scale such as extratropical and tropical cyclones) as having one or more of the following: tornadoes, winds equal to or exceeding 25.8 ms^{-1} , or hail 2.5 cm or greater in diameter (Bluestein 2013). In the past decade, tornadoes have caused more than \$14.1 billion in total damage across the United States (US). Besides, from 2010 through 2020, tornadoes resulted in \$2.5 million in property damage per storm in US. According to another report, storm-related loss has a share of \$171B of \$476B in total economic losses due to meteorological damages in the last 50 years only in Europe (WMO 2021). It is known that tornadoes and convective/frontal storms play a major role in a significant part of these. Nevertheless, economic losses due to only hail, tornado and lightning in twenty-first century is \$11B only in Europe (WMO 2021).

Extreme weather events such as floods, droughts, heat waves and tropical cyclones are related to the climate and somehow linked with the recent global climate change. Furthermore, it is difficult to state that each and every one of the events is an indication of a change in the climate. Extreme weather events can be separated in two groups: firstly, weather-based events relatively short-termed events which can be predicted 1–2 weeks ahead such as tropical cyclones, severe floods, etc., secondly, climate-based events such as drought, season-long heat waves, multiple occurrences of severe storm events and record wildfire (Diaz and Murnane 2008). Extreme weather events occur due to the complex interactions between large-scale atmosphere–ocean circulation patterns such as the Arctic Oscillation, El-Nino-Southern Oscillation with local weather (Khandekar 2013).

The climate of a region is affected by its geographical location and the geographical features of its surroundings. Large surfaces of land and water such as continents and oceans affect the air mass above it via their radiation balance (incoming, absorbed and reflected radiations). The climate of Türkiye is influenced by four air masses, namely: cP (*Continental Polar, originates from Siberia*), mP (*Maritime Polar; originates from the northern part of Atlantic Ocean*), mT (*Maritime Tropical; originates from the equatorial part of Atlantic Ocean, Mediterranean and Aegean seas*), cT (*Continental Tropical; originates from North Africa*) (Türkeş 1996; Sirdas and Sen 2003). Precipitation is an important parameter which is directly affected by the climate of a region. In other way, by using the precipitation data, the climatological characteristics of a region can be determined. Due to its geographical location, Türkiye receives rainfall throughout the year with varying intensity of precipitation over the country, e.g., a city in the East Black Sea region of Türkiye receives 2200 mm of precipitation annually, while another one in Central Anatolia receives only 320 mm of precipitation (Sirdas and Sen 2003; Sirdas et al. 2013).

Precipitation extremes are statistical anomalies of a log-normal probability density function over a region (Sirdas et al. 2013). These extremes have been found to be affected by a plethora of factors, such as sea surface temperatures (SST) anomalies (Grimm and Tedeschi 2009), teleconnection patterns (Vasconcellos and Cavalcanti 2010), synoptic systems like frontal systems (Vasconcellos and Cavalcanti 2010), persistent systems (Carvalho et al. 2002) and large mesoscale convective systems (MCSs) (Durkee et al. 2009) in their study of South American climate. Haylock and Goodess (2004) demonstrated a link between North Atlantic Oscillation (NAO) and extreme precipitation in winter (DJF) by examining two indices of dry-days and wet-day from the data of 347 stations over Europe. A sign of negative NAO has an impact on the storm track in eastern tropical Pacific and western Atlantic (Cassou 2008). Furthermore, this study demonstrates a link between MJO (Madden–Julian Oscillation) and NAO, based on daily geopotential height maps from 1974 to 2007.

The dynamics of moist convection is even more complicated than the already complicated dynamics of dry convection. In mesocyclones supercell environment, the intersection area of cold air from the rear flank downdraft (RFD) region and humid warm air creates wind shear throughout the vertical layer of troposphere. Tornadoes become more likely as streamwise vorticity and storm-relative helicity near the ground increase. According to research, the relative frequency of occurrence of convective hazards such as large hail, severe wind gusts, and tornadoes increases as vertical wind shear increases (Púčík et al. 2021). With deep moist convection tends to become increasingly organized as the vertical wind shear increases (Markowski and Richardson 2011).

The upper-level lows and troughs are responsible for 47% of tornado days and 55% of very large hail days in Türkiye; moreover, nearly a quarter of all synoptic patterns are covered by Mediterranean cyclones with both central and eastern origins, which are well-known and common wintertime events (Kahraman 2021). In fact, the southern and southwestern coastline of Türkiye is likely among the most tornado-prone regions of Europe (Dotzek et al. 2009). For instance, 443 tornado cases were reported on the lands and coastal regions of Türkiye from 2015 to 2022 (Dotzek et al. 2009). There are tornadoes with intensities ranging from F0 to F3, with F1 being the most frequently reported or implied.

Tornadoes, both mesocyclonic and non-mesocyclonic, are most likely to occur in the afternoon and early evening (Kahraman and Markowski 2014; Sirdas et al. 2017). The distinction between waterspouts being non-mesocyclonic and tornadoes being mesocyclonic is rooted in their formation processes. Waterspouts form from smaller-scale interactions over water, while tornadoes are a result of larger-scale mesocyclonic activity within supercell storms. Kahraman and Markowski (2014) revealed that the months of May and June are the most likely for mesocyclonic tornadoes, with October and November seeing a secondary peak in Türkiye. Non-mesocyclonic tornadoes (waterspouts) are most common in the winter along the (southern) Mediterranean coast and in the fall along the (northern) Black Sea coast.

Rasmussen and Blanchard (1998) examined National Weather Service soundings from 1992 to distinguish between environments associated with supercells that produced tornadoes of F2 intensity or higher (deemed “significant” tornadoes), supercells that did not generate significant tornadoes, and non-supercell thunderstorms. In the scope of Mediterranean Basin and especially Türkiye, severe convective storm environments and tornado environments were analyzed comprehensively for the first time and whether revealed to serve the purposes of tornado forecasting (Kahraman and Markowski 2014; Kahraman et al. 2017).

Forecasting convective storms and their attendant hazards, such as tornadoes or large hail, requires knowledge of the characteristics of the environments in which the phenomena tend to occur. Tornadoes have been blamed for at least %4 number of reported economic losses by hazard type around the world (WMO 2021). For this reason, institutions can get rid of high computing costs of numerical modeling if limited area models such as WRF are run for a few days before starting instead of all days to monitor these convective systems operationally. In order to predict these atmospheric conditions, the EMEDO index is developed by using synoptic and mesoscale patterns in the Eastern Mediterranean.

Understanding severe weather environments of tornadic storms in Türkiye will lead to determining mesoscale mechanisms favoring tornadic storms and tornadoes, and these will be some key outcomes of the study not only for researchers, but also for operational forecasters a few days in advance. The purpose of this study is to evaluate and to reveal the connection between a composite Mediterranean Index and tornadic storms.

2 Motivation

In the past four decades, much has been discovered various atmospheric circulations on a local scale that relevant to tornado formation and structure from observations, laboratory models, and numerical-simulation experiments. Nowadays, one of the global climate crisis and adaptation process is to minimize the impacts the severe weather events may cause by utilizing warning systems. At this point, the comprehending and advancing of mesoscale model's studies become particularly crucial in order to predict the formation and dynamical concepts of tornadoes.

Numerous climatic oscillation indices for examining standardized atmospheric pressure fluctuations have been developed, especially focused on the Mediterranean Basin. These include the Mediterranean oscillation (MOi) and the Western Mediterranean oscillation (WeMOi) (Criado-Aldeanueva and Soto-Navarro 2020). Understanding the variability of precipitation has been a focal point in climatic research. The Western Mediterranean oscillation index (WeMeOi), introduced nearly two decades ago, shed light on seasonal variability in western Spain, a phenomenon inadequately explained by the NAO (Martin-Vide and Lopez-Bustins 2006). Building on this foundation, our study introduces the Eastern Mediterranean oscillation index (EMEDOi). Unlike its predecessors, EMEDOi is designed with a specific focus on early prediction of tornadic storms in Türkiye and provides enhanced vertical thickness information throughout the tropospheric layer. These weather events mentioned above, should be taken into consideration several days in advance to assist now-casting approaches. As the early warning systems and alerts should undertake the reducing impacts of severe weather events, the EMEDOi could take a decisive representation in operational meteorology as an indicator of tornado weather. Reliable weather data information combined by conventional weather data and numerical modeling play a crucial role for predicting these sorts of meteorological disasters.

Consequently, there is a need to examine severe weather events in the Eastern Mediterranean region, including Türkiye, and to reveal the clues that the events will take place a few days in advance. At this point, there is a necessity for a composite parameter showing that the atmospheric conditions expected to influence the region will trigger the formation of SCSs (Severe convective storm). Two main hypotheses were determined according to the synoptic characteristics of Türkiye, one of the countries affected by the EMEDOi, which was formed from the points included in the analysis, and in which locations it influenced tornado events.

The results of the analyzes made within the scope of the study and the accuracy of the hypotheses explained below are tested. Firstly, EMEDO_i investigates the induction mechanism of environmental conditions of convective and frontal storm types in favor of tornadoes. Thus, this index reveals the signatures of imminent atmospheric conditions. Secondly, in the scope of the early warning events in terms of presence of low-level pressure systems and extreme weather events, it guides to run the limited area numerical weather prediction models for Türkiye by determining optimum initial model run time in advance.

3 Data and methodology

3.1 Data

In this study, Eastern Mediterranean Basin is the region that covers the main domain of investigation in the area where the composite index is located. Study area has been chosen to let developing of ULL area. Since the frontal movement is a crucial event for the occurrence of mesocyclonic events and synoptic events, the points in the domain have been chosen to consider different regions, respectively. The main domain is limited between 25°–50° N latitudes and 0°–50° E longitudes. The analysis focuses on the Mediterranean Basin (particularly the eastern part) as a limited area model domain, and it contains five different selected grid cell points (Fig. 1, Table 1).

The GDAS (Global Data Assimilation System) re-analysis dataset by the GFS model of the National Center for Environmental Prediction (NCEP) has been used (Table 2). In addition to that, data are utilized as initial conditions and to establish pre-analysis of tornadic storm events and until several hours later. It has 6-h temporal resolution and 0.25° spatial resolution, and it covers 20,301 total grids as 201 grid points west to east and 101 grid points south to north with 27 km (0.25°) spatial resolution. For the map visualizations and diagrams, a few of smoothing processes were applied. These data consist of geopotential (m^2s^{-2}) for specific limited area model domain.

In addition, 14 tornado events (Table 3) and 1 hail event are selected to investigate EMEDO index while 5 events as a test cluster were added to ensure that the index was stable (Table 4).

3.2 Methodology

The EMEDO_i is a barometric pattern index measuring over the Eastern Basin of the Mediterranean of fluctuations in the pressure difference at upper-level troposphere between the Israel and the triangle area in the vicinity of Greece/Albania (Fig. 2).

According to hydrostatic equilibrium equation, geopotential unit is in m^2s^{-2} as in the following equation (Eq. 1):

$$\Phi(z) = \int_0^z g \partial z \quad (1)$$

The geopotential unit was divided by the gravitational acceleration at the surface of Earth (g_0) due to the application of hydrostatic equilibrium in the atmosphere, to convert the data set into a geopotential height as in the following equation (Eq. 2).



Fig. 1 Representation of oscillation points in analysis domain over Eastern Mediterranean Basin (Inclined Satellite Projection)

Table 1 Oscillation points

Geospatial point (defined location)	City, Country	Latitude, Longitude—(DD)
<i>P0</i>	Ashdod, Israel	31.81 N, 34.65 E
<i>P1</i>	Lecce, Italy	40.35 N, 18.18 E
<i>P3</i>	Durres, Albania	41.31 N, 19.46 E
<i>P4</i>	Ioannina, Greece	39.67 N, 20.86 E
<i>C</i>	Vlore, Albania	40.46 N, 19.48 E

Table 2 Description of model configuration and utilized data

Model	GDAS
Central point of domain	Ashdod, Israel
Spatial resolution	27 km (interpolated to 13.5 km)
Vertical level	23+ (4 levels are used)
Temporal resolution	6 h (interpolated to 3 h)
Temporal extent	01.01.2017 00:00 UTC to 31.12.2022 23:00
Initial/boundary conditions	Arranged by GFS, NCEP-NOAA

$$Z = \frac{\Phi(z)}{g_0} \tag{2}$$

Weather parameters are favorable for the occurrence of strong storms and tornadoes as follows; conditionally instability, moisture, frontogenesis, CIN, CAPE, equivalent potential temperature, LCL, LFC, etc. Development of strong storms indicates sharp changes in meteorological conditions which this is steady larger frontogenesis adjacent to tornado location. Observed tornado cases indicates air masses convergence each other and generating larger frontogenesis.

Frontogenesis is the process by which a front form, and it typically occurs when two air masses with different properties encounter each other. As the air masses interact, they begin to move and mix, and this can cause the formation of a front. Frontogenesis occurs when the temperature and humidity gradients across the front become stronger, leading to the development of a more distinct and well-defined front. Fronts and frontogenesis are important because their structures can specify a key role in the development of weather systems, such as thunderstorms or snowstorms. Besides, frontolysis refers to the process of a frontal boundary breaking down or dissipating, while frontogenesis refers to the opposite process, in which a frontal boundary forms or strengthens. Equation 3 indicates the 2D kinematic frontogenesis of a temperature field.

$$F = \frac{1}{2} [|\nabla\theta|(D\cos(2\beta) - \delta)] \tag{3}$$

F is 2D kinematic frontogenesis.

θ is potential temperature.

D is the total deformation.

β is the angle between the axis of dilatation and the isentropes.

δ is the divergence.

Table 3 Selected tornado/waterspout events for training in Türkiye and their features

Date	Time (UTC)	Latitude/Longitude	Intensity	Path length (km)	Path width (m)	Funnel cloud	Area	Province
17.01.2016	16:00	36.26 N, 29.99 E	F1	7	270	Yes	Landwater	Antalya
05.02.2016	13:30	36.91 N, 30.57 E	F1	?	?	?	Land	Antalya
03.03.2016	15:00	36.80 N, 31.49 E	F1	?	?	Yes	Land	Antalya
13.11.2017	18:30	36.34 N, 30.19 E	F3	8.1	300	Yes	Land	Antalya
21.11.2018	10:05	36.82 N, 28.31 E	F1	?	?	Yes	Waterland	Mugla
24.01.2019	10:30	36.36 N, 30.28 E	F2T4	9	400	Yes	Landwater	Antalya
26.01.2019	07:58	36.89 N, 30.80 E	F2T4	11.2	360	Yes	Waterland	Antalya
06.01.2020	17:10	36.59 N, 31.88 E	F1	?	?	?	Land	Antalya
08.10.2020	10:20	40.98 N, 27.98 E	F0	?	?	?	Water	Tekirdag
27.01.2021	05:30	36.75 N, 28.99 E	F1	?	?	?	Land	Mugla
11.02.2021	18:10	38.26 N, 26.38 E	F2	3.3	100	?	Waterland	Izmir
12.10.2021	11:45	37.40 N, 27.65 E	F1	?	?	?	Land	Mugla
07.12.2021	07:33	38.24 N, 26.31 E	F1	3	110	?	Landwater	Izmir
19.12.2021	11:12	36.62 N, 31.77 E	F1	?	?	?	Waterland	Antalya

Copyright by European Severe Storms Laboratory (Dotzek et al. 2009)

Table 4 Selected tomado/waterspout events for stability test in Türkiye and their features. Copyright by European Severe Storms Laboratory (Dotzek et al. 2009)

Date	Time (UTC)	Latitude/Longitude	Intensity	Path length (km)	Path width (m)	Funnel cloud	Area	Province
09-01-2022	18:20	36.30 N, 30.33 E	F0	?	?	?	Waterland	Antalya
02-03-2022	17:35	36.96 N, 31.05 E	F1	5	220	?	Land	Antalya
19-04-2022	06:30	36.84 N, 31.18 E	?	?	?	?	Waterland	Antalya
15-10-2022	06:00	36.70 N, 31.51 E	?	?	?	?	Water	Antalya
07-11-2022	09:00	36.57 N, 31.87 E	?	?	?	?	Water	Antalya

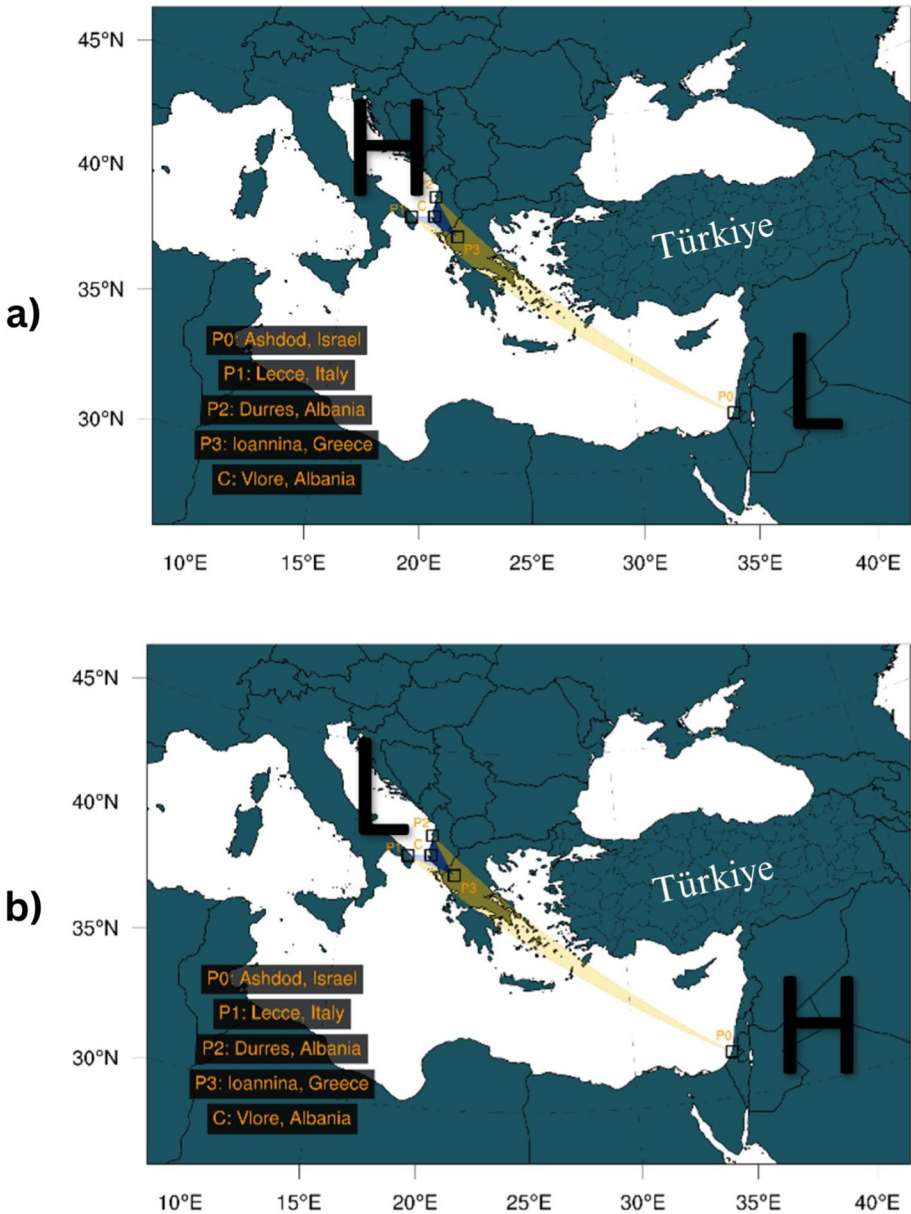


Fig. 2 Representation of oscillation points in analysis domain (Lambert Projection) and pressure placements indicates positive EMEDO index (top) and negative EMEDO index (bottom)

The equation is used to identify frontogenesis and frontolysis over Eastern Mediterranean on the maps.

EMEDO_i values were divided into two phases as EMEDO_i (–) and EMEDO_i (+), thus the effect of either phase on the climatic parameters, as mentioned below, were

detected and compared. The EMEDO_i was expressed by (Eq. 4) which are consists of two different parts in (Eqs. 5) and (6):

$$\text{EMEDO}_i = \text{ThkCoef} \times \text{UL pattern} \tag{4}$$

$$\text{ThkCoef} = \mp \frac{(Z_{500} - Z_{1000})_i - (Z_{500} - Z_{1000})_{P_0} - \text{cf}}{15} \tag{5}$$

$$\text{UL pattern} = \frac{|Z_{500_i} - Z_{500_{P_0}}|}{20} \times \frac{|Z_{300_i} - Z_{300_{P_0}}|}{20} \tag{6}$$

for $i = P1, P2, P3$ from Table 1 and correction factor (cf) = 10.17.

The coefficient part of the formula, “ThkCoef,” indicates fluctuations in the geopotential height thickness between 1000 and 500 hPa isobaric levels. It should also be considered that the coefficient part determines whether or not the EMEDO_i has positive or negative sign. The main part of the formula, which is called the “UL pattern,” demonstrates the upper-level synoptic pattern surrounding air around 500 hPa and 300 hPa.

The EMEDO_i poles, unlike specific pressure centers like the Icelandic Low or Azores High, are influenced by a combination of factors, including Rossby waves and subtropical/tropical air pressure sequences. These dynamics play a role in how dominant pressure systems impact the regions. Due to global warming stems from surplus of energy budget of the Earth, it should be considered that extending high pressure areas at around 30 N/S latitudes due to radiative energy surplus. Take into consider these conditions, P₀ pole has mostly greater thickness difference than the triangle area which is located in the norther during the seasons. Thus, it leads constant thickness difference between two poles of EMEDO_i. In order to prevent inconvenient analysis, correction coefficient is produced for H500–H1000 geopotential height on annual data of 1991–2020 period climatologically. This adjustment value indicates the mean difference of last 30 years between index poles. It helps to compensate this deviation between two different poles of EMEDO_i.

3.3 Variations of EMEDO_i

There are seven (three main, one control, one maximum, one ensemble means, and one operational) variants of EMEDO_i. The necessity for EMEDO-Control (EMEDO-Ctrl) is related to point 3 and investigates the existence of a trough over Greece and aids in understanding the structure of the trough over Greece, including whether or not it has cut-off or moving extension of Rossby waves. In this way, EMEDO-Oper is derived from the coefficient of computation of the main fluctuations (EMEDO₁, EMEDO₂, EMEDO₃, and EMEDO-Ctrl). In addition to these, EMEDO-Max corresponds to at least one point where the values are at an extreme level. Besides, EMEDO-Ens represents the total strength of the fluctuations. When cutoff low-pressure system dragged from southwest to northeast direction, one of the points in the triangle allows to detect the transition of low-pressure system.

$$\text{EMEDO}_i = \text{ThkCoef}_i \times \text{UL pattern}_i \tag{7}$$

$$\text{EMEDO}_{\text{ctrl}} = \text{ThkCoef}_c \times \text{UL pattern}_c \tag{8}$$

Fig. 3 Geopotential height [gpdam] at 300 hPa (isohypses) and geopotential height [gpdam] difference between 500 and 1000 hPa (shaded color contours) **a** 27.01.2016—12 UTC; **b** 16.02.2017—18 UTC; **c** 21.03.2020—00 UTC

$$\text{EMEDO}_{\text{oper}} = \text{ThkCoef}_c \times \text{UL pattern}_{\text{mean}} \quad (9)$$

$$\text{EMEDO}_{\text{ens}} = \text{ThkCoef}_{\text{mean}} \times \text{UL pattern}_{\text{mean}} \quad (10)$$

$$\text{EMEDO}_{\text{max}} = \text{ThkCoef}_{\text{max}} \times \text{UL pattern}_{\text{max}} \quad (11)$$

for $i = P1, P2, P3$ and $c = C$ from Table 1.

EMEDO is in a positive phase with stronger air pressure in the middle of the Mediterranean Sea and southern Europe than average. During the positive phase of EMEDO_i, geopotential thickness decreases due to ULL's movement toward lower latitudes. Azores high-pressure system changes its position and extends horizontally to the northeast. This high pressure is stagnant around the middle Mediterranean Basin and replaces the pressure in Mid-Europe. In this way, EMEDO_i becomes strong in its positive phase. The increased difference in pressure between the two regions leads to an enhanced ridge in southern Europe. There is an extremely eastward shift of the storm track during positive EMEDO phases. Israel's vicinity (the Harbor of Ashdod) is influenced by humid and cold air masses or cyclones. These air masses are typically dominant and stem from a tributary of the Indian monsoon. Consequently, southern Europe experiences decreased storminess and precipitation and warmer-than-average temperatures that are associated with the air masses that arrive from higher latitudes. In western Türkiye, the positive phase of the EMEDO generally brings stagnant higher air pressure; a condition associated with fewer cold air outbreaks in the following days and decreased storminess. At the same time, the Middle East and Caspian Sea experience lower-than-average temperatures, increased storminess, and above-average precipitation. Hence, ULL brings wet weather across the Middle East. Besides, the ULL movement through the Mediterranean Sea should be considered due to the moving of Rossby waves to the east as a requirement of middle latitudes in the Northern Hemisphere. As a result, the positive phase of EMEDO_i is mostly observed as a regular movement pattern of pressure sequence after the negative phase (Fig. 3).

The EMEDO_i's negative phase is characterized by lower-than-average air pressure with baroclinic conditions over the mid-southern Mediterranean Basin. The jet stream is directed from southwest to northeast under these conditions with the contribution of upper-level trough. In winter, the Azores high affects Western Europe, triggering EMEDO's influence in the Eastern Mediterranean. This leads to intense ULL systems and snowstorms in areas like Greece and Türkiye. EMEDO's negative phase correlates with heatwaves in the Western Mediterranean and decreased storminess. In other words, a negative EMEDO_i phase is associated to northern based airflows which have traveled and get humidity over the Mediterranean Sea; these are therefore laden with moisture when they reach the Crete and Rhodes Islands of Greek Islands, western side of the Türkiye, leading to increased (sometimes torrential) frontal precipitation in this area. Tornadoes are more frequent across Eastern Mediterranean and along with coasts of Greece and western parts of Türkiye. These events are typically caused by either supercell frontal structures on the MCS line or sea-induced instabilities which is necessary for waterspouts in Fig. 4.

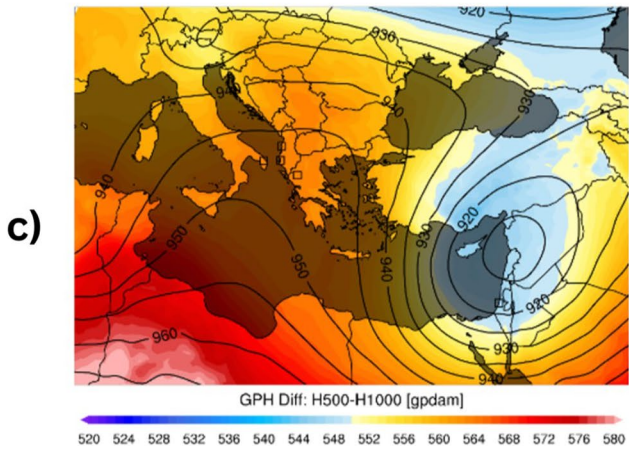
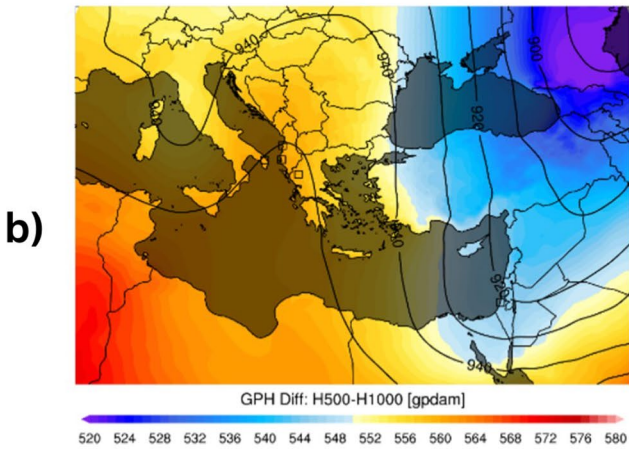
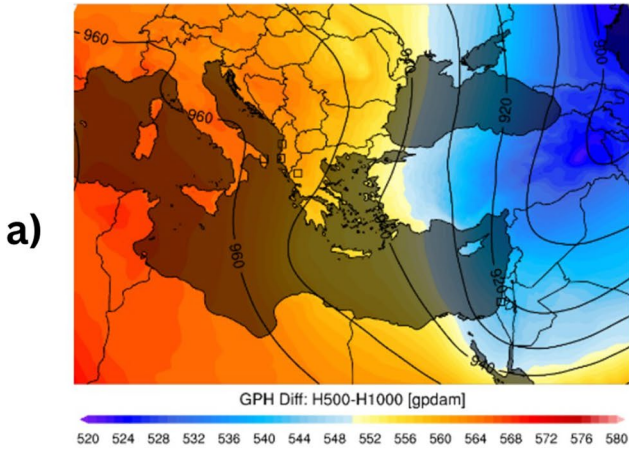


Fig. 4 Geopotential height [gpdam] at 300 hPa (isohypses) and geopotential height [gpdam] difference between 500 and 1000 hPa (shaded color contours) **a** 21.04.2017—12.00 UTC; **b** 23.03.2018—18 UTC; **c** 22.03.2021—18 UTC

4 Results and discussion

Storm tracks are formed throughout the North Atlantic as a result of jet streams in the troposphere, which are responsible for the separation of distinct air masses and the resulting gradients in temperature, precipitation, and other factors. The jets are relatively undulating and buckles the pattern changes. Because of the movement of these patterns carried on by westerlies, numerous air masses have been positioned zonally and meridionally over Europe. Therefore, on the European continent, high pressure over Scandinavia which are called Scandinavian Block, which can occur with the development of the Atlantic Ridge (AR), is an example of pressure settlements that can cause the EMEDO index to decrease. That is because, much stronger jets tend to be propagated across the Mid-Europe and hold the area of Eastern Mediterranean which allows of deepening the ULL and winds strengthen. On the other hand, Greenland Block can cause the development of low-level pressure system around contiguous Europe which is able to keeps the North-western Europe countries within the colder airflow coming from Polar region. This settlement may result in a little ridge of high pressure over middle Mediterranean and it increase the value of EMEDO_i to positive phase.

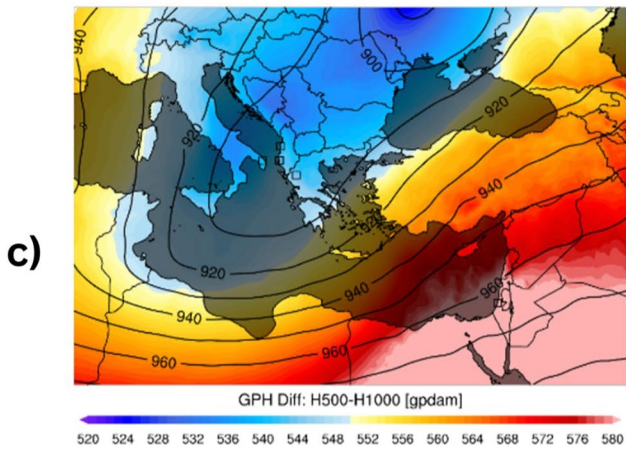
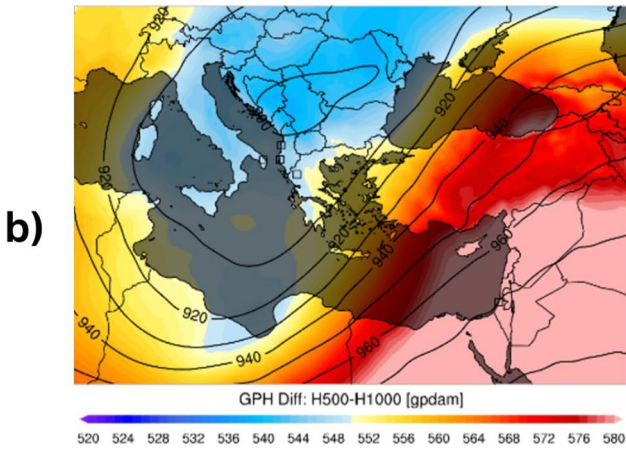
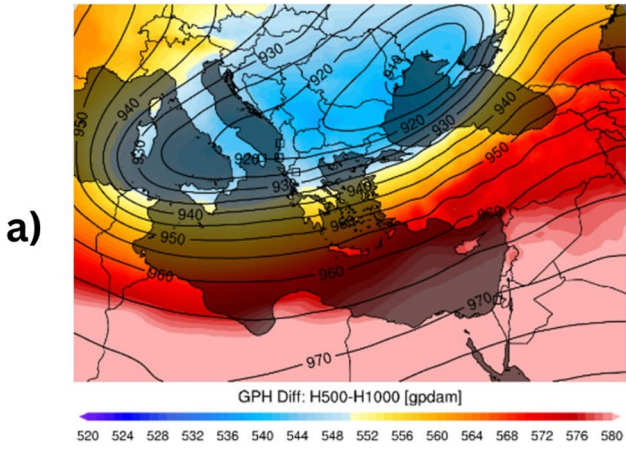
One of the primary drivers for convective storms, capable of spawning tornadoes, is the availability of moisture in the lower atmosphere. Changes in large-scale atmospheric circulation patterns in terms of geopotential can also impact the frequency and intensity of these storms. In particular, when the Azores High evolves into the Scandinavian Block (BLO+) via North-western Europe, it creates a conducive environment for frontal and convective storms over the Eastern Mediterranean, including Greece, Cyprus, and Türkiye. This high-pressure system promotes a convergence area and upper-level low (ULL) pressure system over Mid-Eastern Europe, curving the jet stream downwards and triggering the flow of cold air through southern latitudes.

Sharp temperature gradients at cold and warm front boundaries can lead to super-cell thunderstorms, the primary producers of intense tornadoes. Our analysis showed that such atmospheric conditions are especially prominent in the Euro-Mediterranean region during the northern hemisphere winter, commonly occurring from October to May (Fig. 5).

Besides all these, a negative skew will indicate a tail on the left side and will extend to the more negative side. According to the analysis of Fisher-Pearson standardized coefficients, EMEDO_i has severe left skewness for all the year periods and they should be optimized to have normal distribution, or the formula might be updated (Fig. 6). EMEDO_i of all year periods has been observed that the distribution has a thicker left tail and mode > median > mean.

The all variation of EMEDO indices were analyzed in the range of 10 days which is from 5-day before ($t-5$) to 4-day after ($t+4$) the event day. The figures plotted below, which are based on geopotential heights and frontogenesis additional to the EMEDO indices, will be used to examine 14 separate tornado events (trained clusters) according to their EMEDO indices local minimum times.

Among the 14 tornado incidents that took place in different years, three are considered prominent. In this incident (Figs. 7, 8), ULL entering from a narrower area created a relatively strong positive vorticity advection. The EMEDO-Oper value reached a magnitude



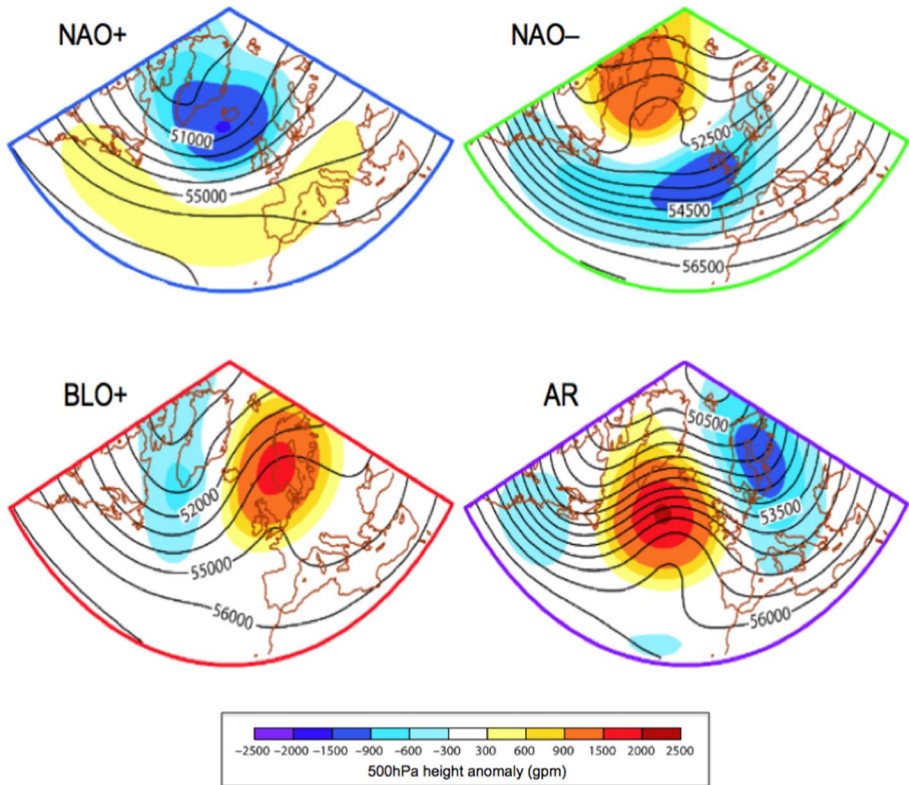


Fig. 5 Diagrams depict the Euro-Atlantic sector around which the regime definitions of geographical patterns of Euro-Atlantic climatological regimes (both anomalies and full fields) as used at ECMWF. North Atlantic Oscillation, positive phase (NAO+), North Atlantic Oscillation, negative phase (NAO-), Blocking (BLO+), The Atlantic Ridge (AR) circulation pattern is a particular case of Anti-blocking (BLO-), in which the important feature is the trough over Scandinavia. Geopotential anomalies (color shading) and geopotential (contours) at 500 hPa are shown (Cassou 2010). Copyright by European Centre for Medium-Range Weather Forecasts

less than -4 and persisted around this value for approximately 12 h (Fig. 9). It is possible to interpret this as the trough gathering strength and remaining motionless. The hour when the hose came out occurred during the hours when the EMEDO values started to decrease with a high tendency value. Lower geopotential heights around the surrounding air are indicated on one of the reference points at the western polar caps. Prior to the event, the EMEDO-Max value was less than -6 . And when the graph is examined carefully, it is clearly seen that the EMEDO-Oper index value, which is almost reaching the value of -5 , returns to the neutral phase within 24 h. This shows us that the ULL, which was stagnant at first, moved rapidly to the east in the following hours.

The most important difference of this system is that the main ULL zone is located further west than the EMEDO western pole (Figs. 10, 11). Although it seems like a skeptical system synoptically, the EMEDO-Oper value approached -1 in condition that produced the most severe event of recent years at the F3 intensity level (Fig. 12). Also, in this incident, a low-pressure system with semi-cutoff support, which moved with the front on the Mediterranean, left the main system and struck Türkiye again from

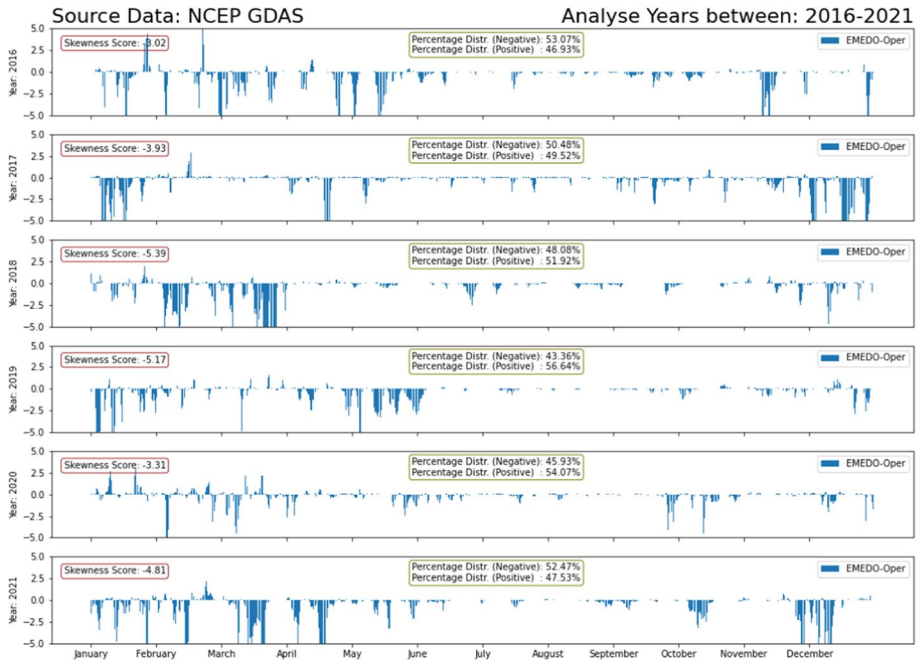


Fig. 6 Values of EMEDO-Oper indices (the vertical axis) in 6-h temporal resolution during based on the years of 2015–2021 climatological period (the horizontal axis), percentage distributions of EMEDO_i during the years (upper center), and adjusted Fisher-Pearson standardized moment coefficients (upper left)

Africa. The fact that the tornado, which emerged during the decrease in tendency, fell to a height of 900 gpdam at the jet level reveals that the groove hit Türkiye in a fragmented manner.

The SCSs that occurred in this and the following week were triggered by systems where the jet level temperature gradient between the EMEDO poles was strongest (Figs. 13, 14). The EMEDO-Oper index, which almost approached the -3 value, passed into the neutral phase within 18 h and one of the fastest transitions between ULL systems was observed (Fig. 15).

There have been observations made of patterns that may be understood to be shared by all EMEDO_i members. Before tornadoes occur, the oscillation pattern and circulation of EMEDO are responsible for explaining many of the meteorological characteristics. The geopotential heights that were observed during each incident were distinct from one another because to the pressure drop, the enhanced instability brought on by the presence of seawater, and the depth at which the ULL struck Türkiye. This is the essential piece of information necessary to deduce how upper-tropospheric jet streams sweep. The pattern that is frequently observed in all occurrences, with the exception of the one that occurred on March 03, 2016, is that: At the time of the tornado events, the majority of EMEDO_i members (particularly EMEDO-Oper) are predominantly in negative phase. Because of the triangle and center point that were created at the western pole point, cyclones always pass through the Eastern Mediterranean basin on their way to the east. Each incident displayed unique geopotential heights. These variations can be attributed to several factors: the drop in atmospheric pressure throughout the front, the

Frontogenesis: 925 hPa
Unit: [K/100km/3h]

GDAS (Analyse)
2016/02/04 - 18:00 UTC

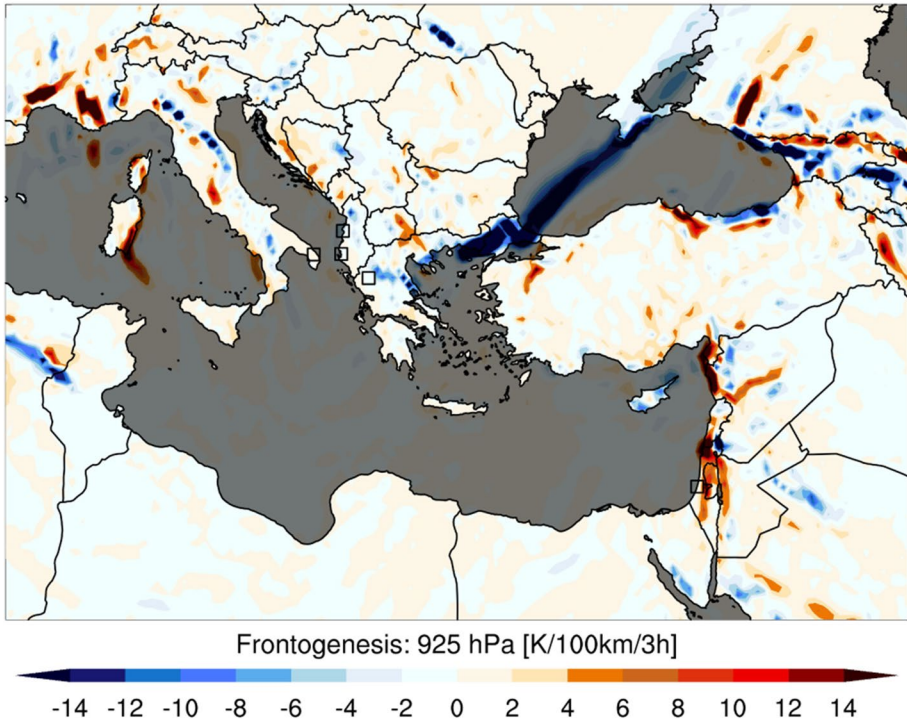


Fig. 7 Near-surface (925 hPa) horizontal frontogenesis function [K/100 km/3 h]

increased instability due to the presence of seawater, and the depth at which the upper-level low (ULL) impacted Türkiye. Understanding these variations is crucial for interpreting the behavior of upper-tropospheric jet streams.

A consistent pattern was observed across most events. Except for the incident on March 03, 2016, during the tornado occurrences, the majority of EMEDO_i members, especially EMEDO-Oper, were predominantly in a negative phase. The specific configuration of the triangle and center point at the western pole ensures that cyclones typically traverse the Eastern Mediterranean basin on their journey eastward. Because of this, they always cause a decrease in thickness near the ground and a decrease in geopotential height in the upper troposphere. The reason for this can be explained by the fact that the triangle and center point were created at the western pole point, which corresponds to the north-western part of the shaded area in Fig. 1.

At the time of the tornado, the EMEDO-Oper value is typically in a negative phase. This is applicable to the majority of the selected tornado incidents. At the time of the tornado occurrence, the values of this member can only possibly qualify as being in a neutral phase in two plots that make up a relatively insignificant portion of the train cluster. In the negative EMEDO phase, the geopotential gradient deepens between the trough over Italy, Greece and Albania and the ridge in the vicinity of Israel; as a result, the environmental conditions in the Eastern Mediterranean are more favorable for the formation of a frontogenesis. In addition, the strength of fronts was typically

GPH: H300 [gpdam]
 GPH: H500-H1000 [gpdam]

GDAS (Analyse)
 2016/02/04 - 18:00 UTC

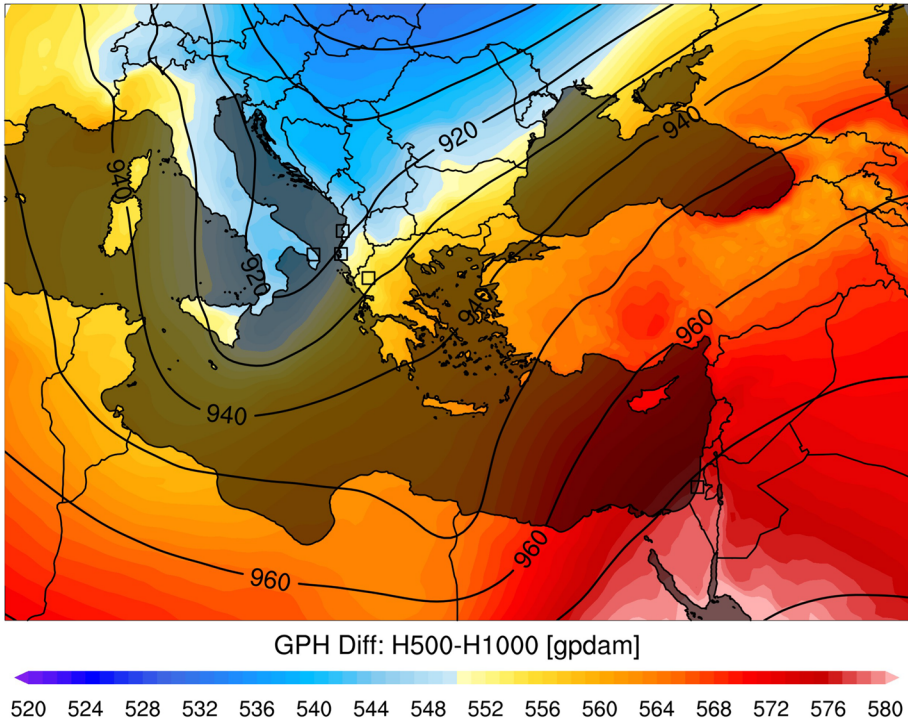


Fig. 8 Geopotential height [gpdam] at 300 hPa (isohypses) and geopotential height [gpdam] difference between 500 and 1000 hPa (shaded color contours)

characterized as being in the strong classification, which is described as having more than 8 K per 110 km of gradients (Sanders 1999). There have been a few instances of events that have been reported as waterspouts, and in those instances, the power of the fronts has been classified as moderate (4 K/110 km).

The hourly period until the local minimum is obtained can be described and characterized as the process by which the EMEDO-Oper index value decreases continuously. Therefore, the procedure for achieving the local minimum varies between events. This period is calculated to be an average of 31.3 h based on the tornado occurrences in the Train Cluster, and 33.2 h when the 2022 tornado occurrences are included.

This procedure varies based on the velocity of the incoming trough, which transports cold air from the high latitudes to the Mediterranean. Systems located in the Central Mediterranean linger in the Italy–Albania–Greece triangle (*P1*, *P2*, *P3*, respectively), sometimes due to Omega blockade and other times because to cyclonic cut-off obstructions emanating from the dipole. Such instances demonstrate how long the ULL, which is a component of the EMEDO-Oper index, lingers in the region of western pole of EMEDO_i, and how the eastern pole over Israel contribute to the increase in values caused by the presence of high pressure and ridge effect. Thus, EMEDO-Oper values might remain in the negative phase for an extended period of time and grow stronger.

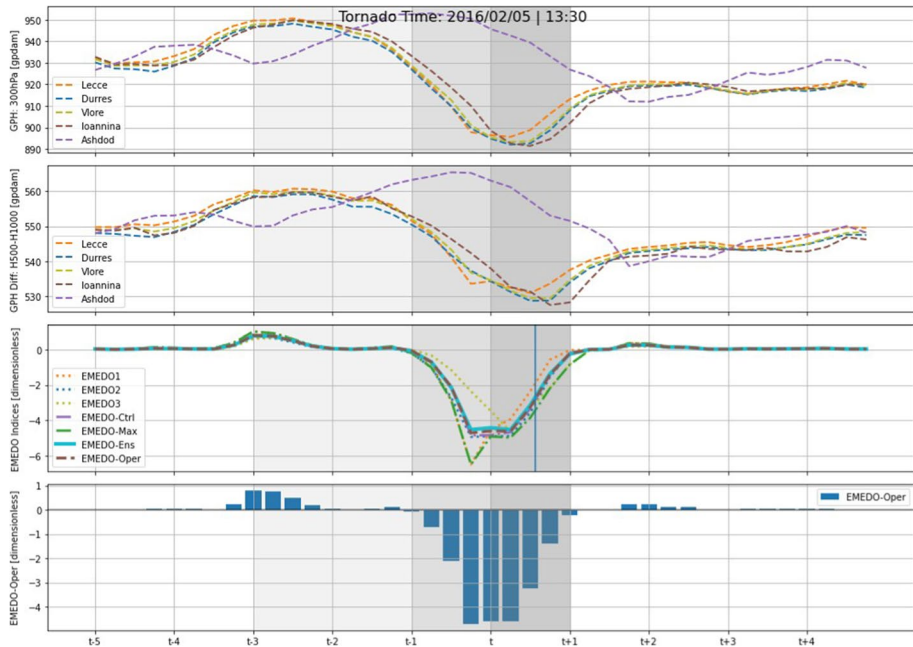


Fig. 9 10-days all EMEDO member oscillations (the vertical axis) surrounding tornado incidents in daily period (the horizontal axis) (05.02.2016). The lightest shaded areas indicate 1 to 3 days before the tornado event of EMEDO_i members; whereas, the darkest shaded parts indicate the days when EMEDO_i members begin developing negatively. The area with the opaqueness depicts the day of the tornado

In addition, a culminating point may occur at the local minimum point of the negative phase prior to or around the hours of the tornado occurrences, including non-mesocyclonic waterspouts suctioning from warm sea surfaces to relatively cold air at upper-level troposphere. This can take place regardless of the movement of the frontal boundary. There is no set schedule for when a tornado will strike; it might happen at any time. The next portion ought to concentrate on the 72 h that were immediately before the events, with the tornado occurrences serving as the focal point of the investigation. This will allow for a more in-depth analysis in terms of temporal during these 72-h (for instance, t-24 represents 24-h before the storm time).

5 Evaluation of results

Examining the variations of the numbers 1, 2, and 3 of EMEDO_i reveals that the number of extreme values and values that can be regarded outliers is smaller than the variations of control, ensemble, operational, and maximum (Figs. 16, 17). When all variances are taken into account, the average values measured roughly -3 and achieved a local minimum 12 h before to the tornado events (Fig. 18). The median values, on the other hand, maintained the same overall oscillation and decreased below the value of -2.

Although the box plot lengthens again 12 h after the tornado, this is due only to the synoptic ULL-induced system lingering over the eastern Mediterranean and reducing

Frontogenesis: 925 hPa
Unit: [K/100km/3h]

GDAS (Analyse)
2017/11/13 - 06:00 UTC

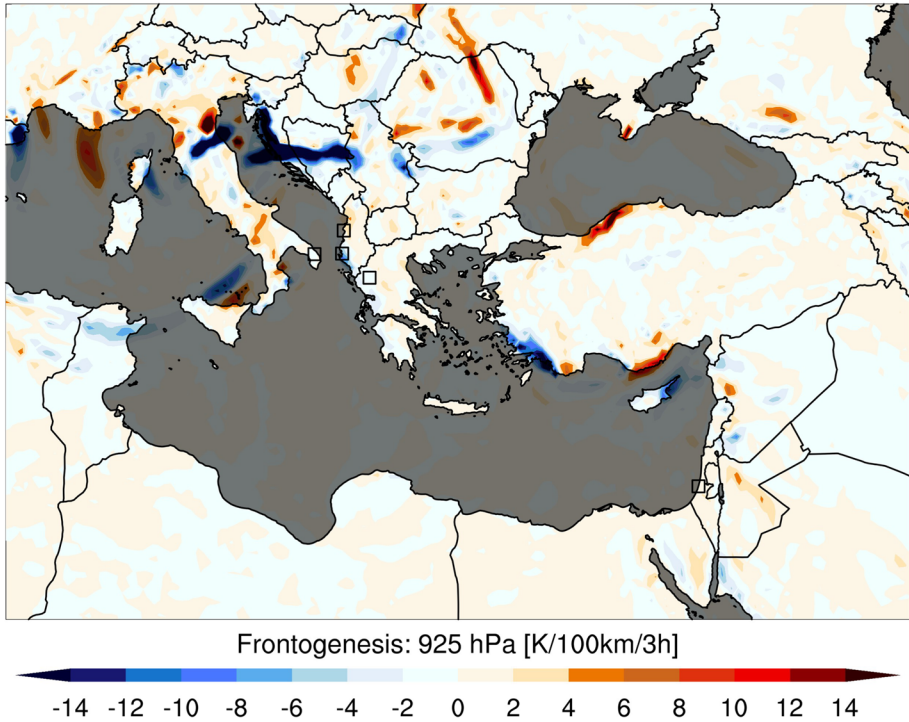


Fig. 10 Near-surface (925 hPa) horizontal frontogenesis function [K/100 km/3 h]

the thickness by generating a reaction low-pressure system over the Mediterranean. This is because as the cold outbreak goes to such southern latitudes, it transforms into the Cyprus Low or the Black Sea Low with cyclonic movement, especially by the water, which remains relatively warm during the winter.

After the tornado has occurred and lost its effect, the response of the EMEDO index values in the negative phase declines at the same rate and approaches neutral. The value of the EMEDO index just prior to the tornado tends to range anywhere from -1 to -4 on average. In addition, while all events oscillate similarly without outliers until 12 h prior to the tornado occurrence, the index values for all events demonstrate significant variations as the tornado time approaches. All variations of EMEDO exhibit the same oscillation patterns.

Moreover, preliminary analysis uses a limited number of cases to explore the potential correlation between negative EMEDO readings and tornado forecasts. Further comprehensive studies are needed to validate the effectiveness of the EMEDO Operational index in tornado forecasting. In the next phase of our research, we will conduct an expanded evaluation of the EMEDO Operational index, which will then be utilized in the subsequent round of study.

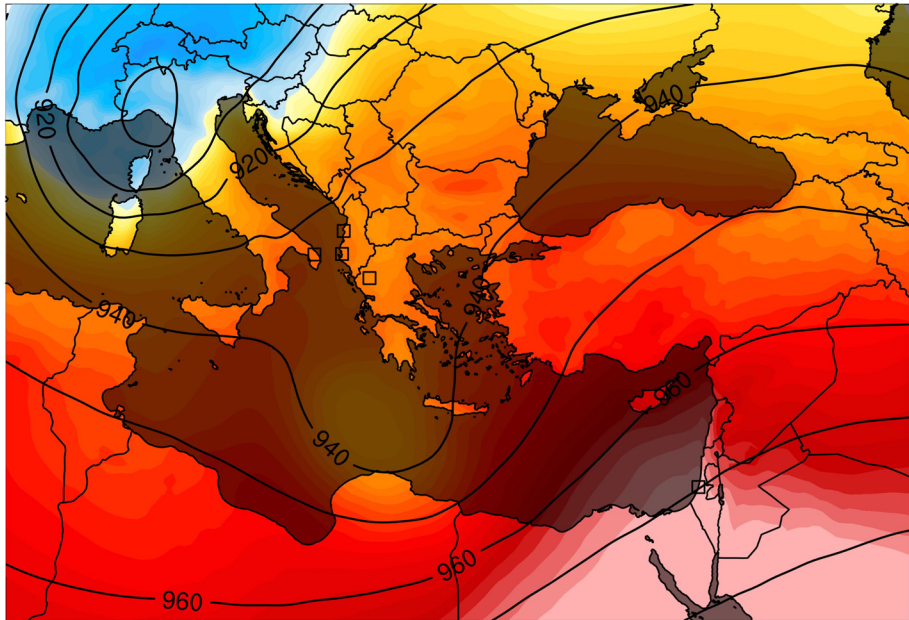
Table 5 refers that the lowest average EMEDO index value was -2.947 12 h before to the tornado. This score indicates the strength of the negative EMEDO_i phase based on whisker plots, where it is a highly remarkable mean. As the tornado approaches, the standard deviation numbers grow. This might be taken as the fact that different systems have

GPH: H300 [gpdam]

GPH: H500-H1000 [gpdam]

GDAS (Analyse)

2017/11/13 - 06:00 UTC



GPH Diff: H500-H1000 [gpdam]

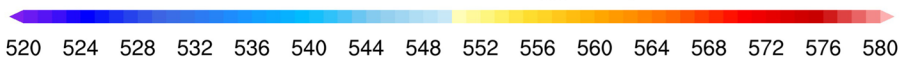


Fig. 11 Geopotential height [gpdam] at 300 hPa (isohypses) and geopotential height [gpdam] difference between 500 and 1000 hPa (shaded color contours)

varying strengths at the index measurement locations; hence, the numbers in the extreme values are excessive.

The minimum value of the EMEDO index is only occasionally lower than -10. These values for the EMEDO index are quite low and are rarely measured. Prior to the occurrence of tornadoes, the minimum values and Pythagorean averages reached the local minimum. In the time series of the 25th, 50th, and 75th quantile values, it is evident that the tendency of EMEDO drops as the tornado approaches and returns to neutral phase following the tornado occurrence. As expected, the highest values are close to 0 because the neutral phase is the period during which the tornado risk is not predicted.

The error values exhibit a pattern that is consistent between t-30 and t-12; however, mean = -0.75 is the value that provides the highest level of accuracy due to the fact that it has the lowest error rates for the entirety of the episode (Fig. 19).

According to descriptive data and box-whisker plots, the average EMEDO index value has attained its local minimum between -0.75 and -3. The MSE and MAE graphs of this index range with 0.25 intervals are as follows in order to establish the reference threshold value. As demonstrated, the error tendency from t-42 to t-30 for reference threshold values is extremely large. The MAE error distribution values range from 0.75 to 2.75. However, particularly between t-30 and t-12, that is, in the section with a shaded backdrop, the appropriate period for the local minimum and whichever index value is used, the margins

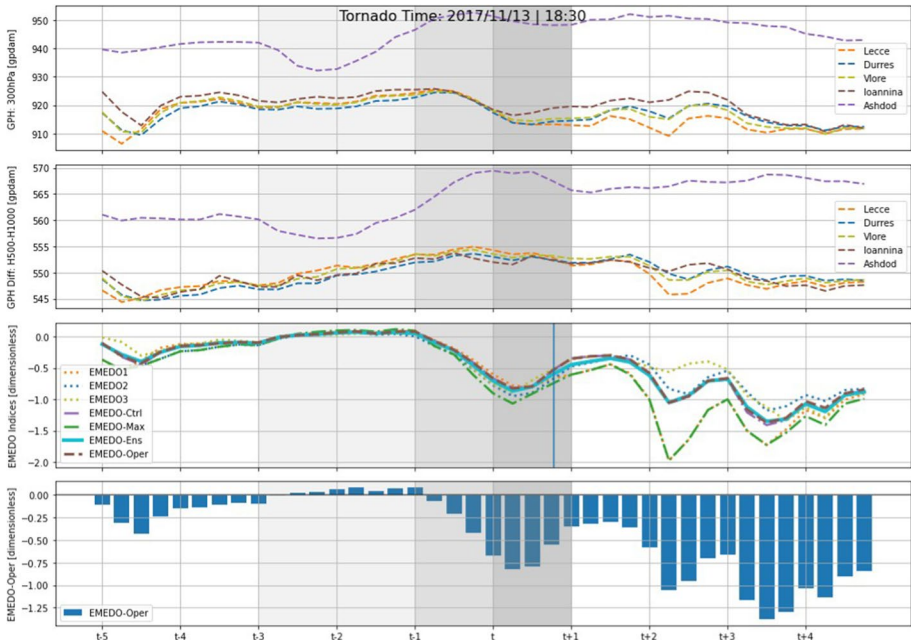


Fig. 12 10-days all EMEDO member oscillations (the vertical axis) surrounding tornado incidents in daily period (the horizontal axis) (13.11.2017). The lightest shaded areas indicate 1–3 days before the tornado event of EMEDO_i members; whereas, the darkest shaded parts indicate the days when EMEDO_i members begin developing negatively. The area with the opaquest color depicts the day of the tornado

of error are quite tight. During this time frame, error rates reach their lowest point, acting like a braid of hair. During this interval, the MAE values do not exceed the threshold of 2, indicating that a tornado is approaching. In addition, error values around the time of tornado events are high for MSE values, while the error values reached their minimum value 30 and 12 h before the tornado.

When the tornado event begins, and the system loses its influence, the error tendency tends to revert to its distribution during the initial time, and error levels rise. The most important finding here is that all lines attain their lowest error levels prior to the tornado, regardless of the threshold values on which the error depends, during the 18-h period indicated by the shaded region. Consequently, the interval between $t-30$ and $t-12$ is crucial for the investigation, and the threshold value as -0.75 will continue to be evaluated because it has the lowest error statistics for predicting the conditions for the occurrence of a tornado event.

As shown in Table 6, for each error distribution of the EMEDO-Oper value, a variety of conclusions can be drawn. Although the MAE value was lower than 1 during the specific time period that occurred 42 h before the onset of the tornado, it rises to a value of 2 as the tornado draws closer, and then it subsequently drops back down to a lower value after the tornado has passed. Due to the negative EMEDO-Oper index, MBE values are calculated as negative during the times around a tornado’s moment. It approaches the 0-limit value 36 h before the tornado and after considerable time. Twelve hours before the tornado, MPE values approach the neutral phase with a value of about 0.1, which can be viewed

Frontogenesis: 925 hPa
Unit: [K/100km/3h]

GDAS (Analyse)
2019/01/24 - 00:00 UTC

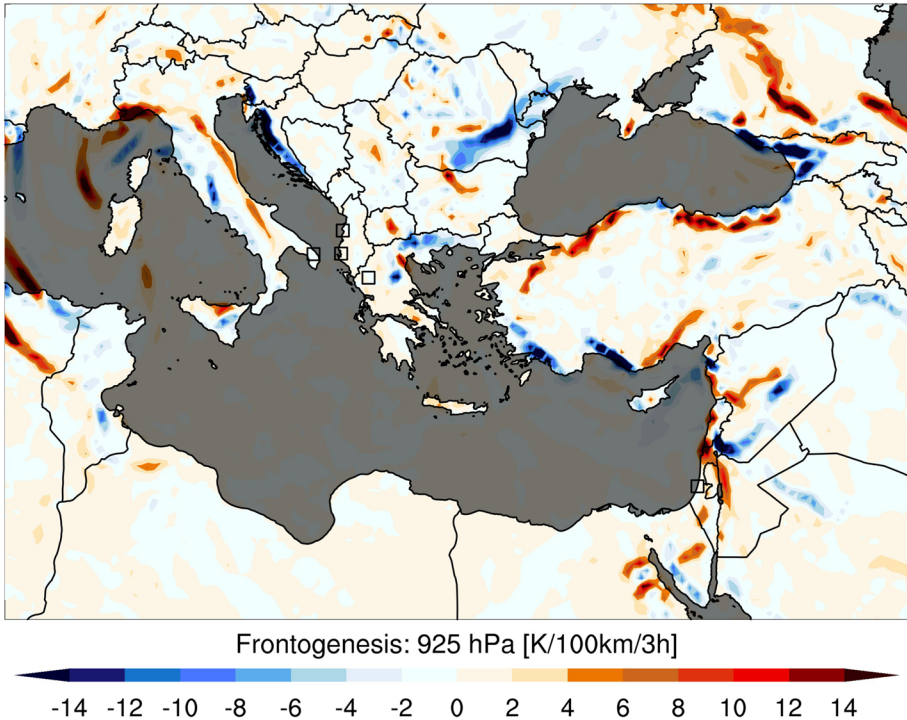


Fig. 13 Near-surface (925 hPa) horizontal frontogenesis function [K/100 km/3 h]

extraordinarily favorably. As indicated in the chart above (Fig. 19), the MSE values were at their lowest between 36 and 12 h prior to tornado occurrences; however, they are exceedingly considerable between $t-18$ and $t+12$.

During the $t-18$ – $t-12$ time frame, the mean absolute percentage error (MAPE) achieved its minimum values before decreasing to roughly 1%. During and after the tornado event, it continued to surge excessively. The error values for root mean square error (RMSE) are at a minimum until $t-18$, a considerable time after the tornado occurrence. Here, the time span $t-18$ – $t+12$ is the interval in which the margin of error is the greatest. Root mean square logarithmic error (RMSLE) has similar tendencies to RMSE.

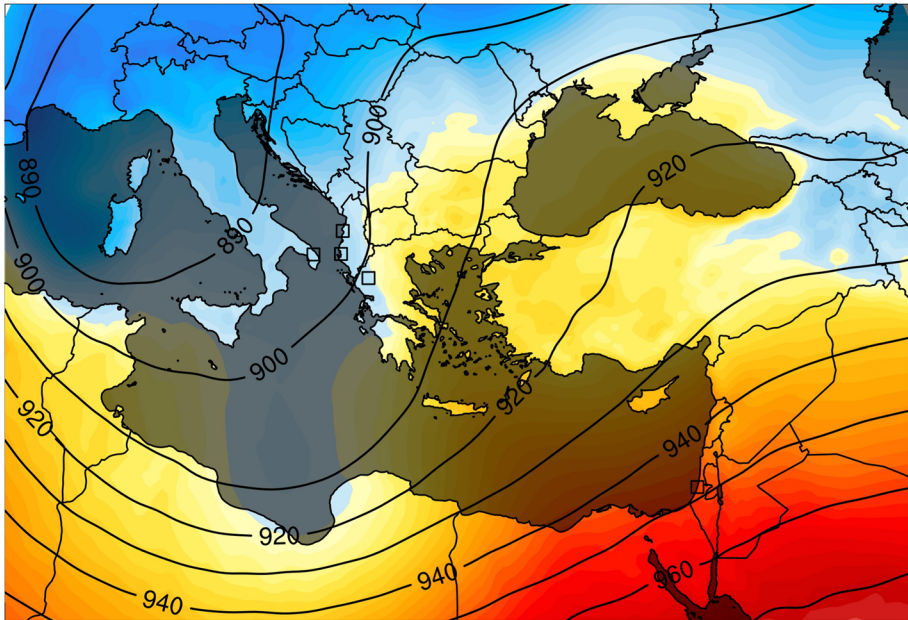
By averaging the correlations between 14 tornado occurrences for the $t-42$ – $t-6$ and $t-30$ – $t-12$ time frames, it is aimed to evaluate whether the EMEDO Operational index is meaningful for all events within the determined local minimum occurrence period. According to Table 7, the success rate in the correlation values for the Spearman variation is evidently between 0.80 and 1 and is calculated as a very significant connection with a high correlation, whereas the Pearson variation typically ranges between 0.60 and 0.80 and can be explained as a strong correlation association. Based on Pearson correlation, the period $t-30$ – $t-12$ exhibited a high correlation, and based on Spearman correlation, the period $t-42$ – $t-6$ likewise exhibited a high relation. Each correlation technique takes a distinct approach to raw data, which is one of the reasons why the scores vary. To clarify, Pearson correlation is a useful metric for normally distributed random variables and linear

GPH: H300 [gpdam]

GPH: H500 - H1000 [gpdam]

GDAS (Analyse)

2019/01/24 - 00:00 UTC



GPH Diff: H500-H1000 [gpdam]

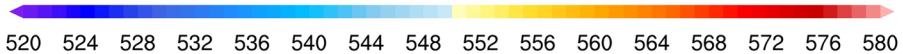


Fig. 14 Geopotential height [gpdam] at 300 hPa (isohypses) and geopotential height [gpdam] difference between 500 and 1000 hPa (shaded color contours)

relationships. However, Spearman rank correlation often describes the skewed link and monotonic relationship between datasets. Therefore, while there is a monotonic relationship over a broad span of time, $t-30-t-12$ represents a linear relationship.

Another objective is to determine if each occurrence provides the right environmental conditions for the creation of tornadic storms in the boundary layer and upper-level troposphere. In addition to that, it generally interacts with the sea in the Eastern Mediterranean atmosphere and modifies the trough’s synoptic characteristics, despite the fact that the majority of ULL systems influence Türkiye in distinct ways. In this manner, it can have a significant impact on coastal provinces in different time zones and months, particularly during the winter.

6 Verification

In this process, an investigation into that severe weather analysis will be carried out employing only EMEDO-Oper for the purposes of operation. Because of this, the five tornadoes that occurred along the western coast of Türkiye in 2022 are detailed in the following sections.

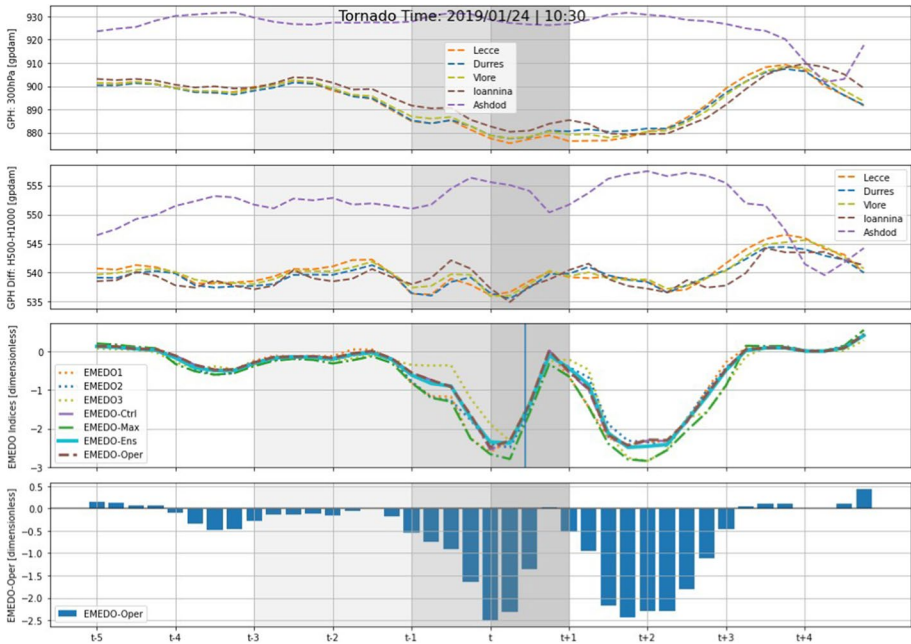


Fig. 15 10-days all EMEDO member oscillations (the vertical axis) surrounding tornado incidents in daily period (the horizontal axis) (24.01.2019). The lightest shaded areas indicate 1 to 3 days before the tornado event of EMEDO_i members; whereas, the darkest shaded parts indicate the days when EMEDO_i members begin developing negatively. The area with the opaqueness depicts the day of the tornado

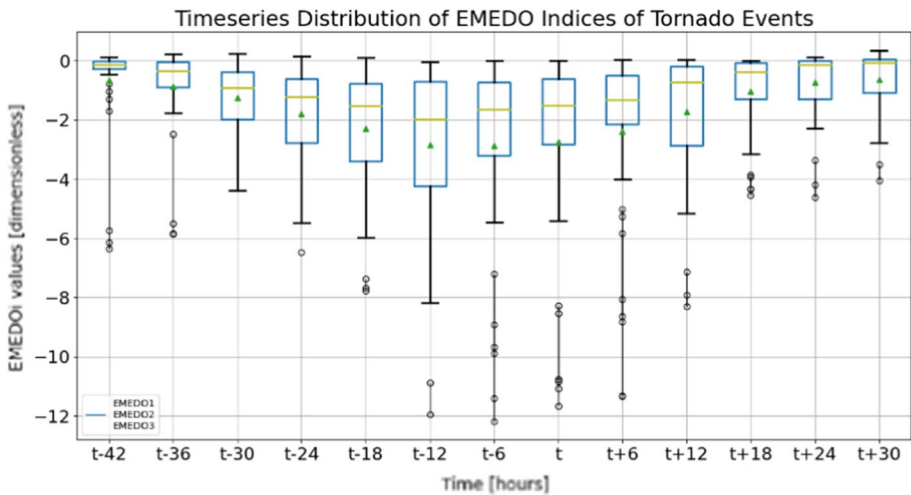


Fig. 16 EMEDO member (1, 2, 3) indices (the vertical axis) in the Whisker-Box plots represent the time period interval (the horizontal axis) of 42 h before to 30 h after tornado events initiated. The boxes extend to the 25th and 75th percentiles, while the whiskers to the 10th and 90th percentiles. Median values are shown as horizontal line within the boxes and mean values are demonstrated as triangle within the boxes

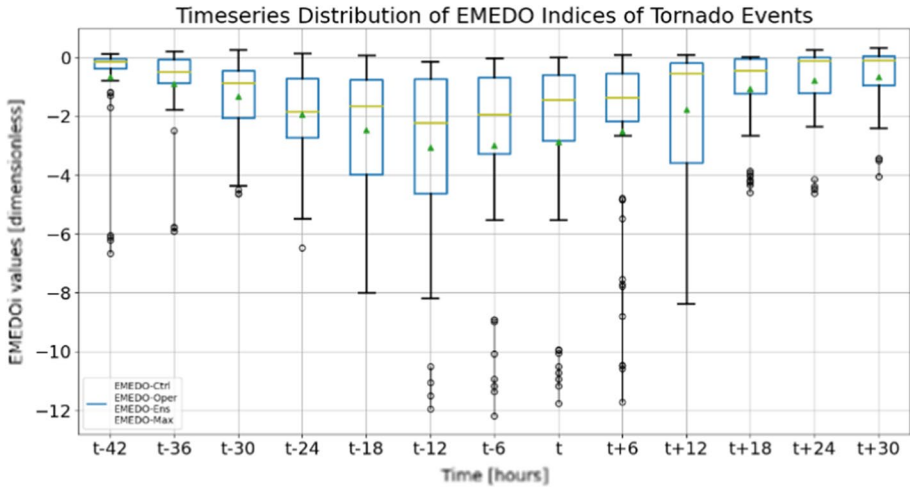


Fig. 17 EMEDO member (Control, Operational, Ensemble, and Maximum) indices (the vertical axis) in the Whisker-Box plots represent the time period interval (the horizontal axis) of 42 h before to 30 h after tornado events initiated. The boxes extend to the 25th and 75th percentiles, while the whiskers to the 10th and 90th percentiles. Median values are shown as horizontal line within the boxes and mean values are demonstrated as triangle within the boxes

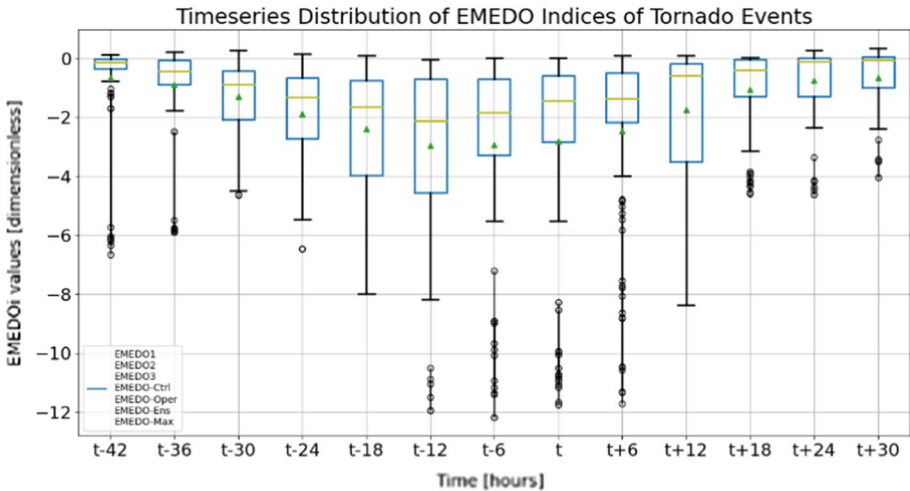


Fig. 18 All EMEDO member indices (the vertical axis) in the Whisker-Box plots represent the time period interval (the horizontal axis) of 42 h before to 30 h after tornado events initiated. The boxes extend to the 25th and 75th percentiles, while the whiskers to the 10th and 90th percentiles. Median values are shown as horizontal line within the boxes and mean values are demonstrated as triangle within the boxes

After statistically validating the EMEDO index, five genuine instances from 2022 were chosen to evaluate the index’s performance. The 14 tornado incidents that occurred in Türkiye over the course of the previous six years were evaluated meteorologically and statistically in order to provide insight into the EMEDO Index’s application. If a

Table 5 Performance statistics of tendency metrics for the differences of EMEDO indices in Türkiye during the period of tornadic storm event

Time	t-42	t-36	t-30	t-24	t-18	t-12	t-6	t	t+6	t+12	t+18	t+24	t+30
Mean	-0.613	-0.832	-1.186	-1.783	-2.267	-2.947	-2.853	-2.751	-2.411	-1.682	-1.011	-0.74	-0.623
Geometric mean	-0.129	-0.318	-0.597	-0.987	-1.382	-1.646	-1.297	-1.183	-1.023	-0.475	-0.182	-0.153	-0.197
Harmonic mean	-0.052	-0.097	-0.138	-0.182	-0.596	-0.837	-0.161	-0.178	-0.216	-0.105	-0.011	-0.033	-0.062
Standard deviation	1.596	1.499	1.223	1.416	2.041	3.119	3.346	3.453	3.118	2.333	1.423	1.242	1.098
Min	-6.039	-5.791	-4.501	-4.701	-5.981	-11.043	-11.166	-10.732	-10.465	-7.761	-4.173	-4.376	-3.441
Quantiles 25	-0.289	-0.702	-1.912	-2.642	-3.717	-4.197	-3.018	-2.628	-2.06	-2.974	-1.146	-1.08	-0.821
Quantiles 50	-0.069	-0.485	-0.805	-1.629	-1.363	-2.138	-1.754	-1.416	-1.374	-0.509	-0.378	-0.099	-0.078
Quantiles 75	-0.006	-0.078	-0.464	-0.729	-0.724	-0.612	-0.665	-0.687	-0.453	-0.144	-0.048	0.014	0.049
Max	0.055	0.146	0.118	0.017	0.077	-0.167	-0.013	0.015	0.021	0.035	0.009	0.057	0.248

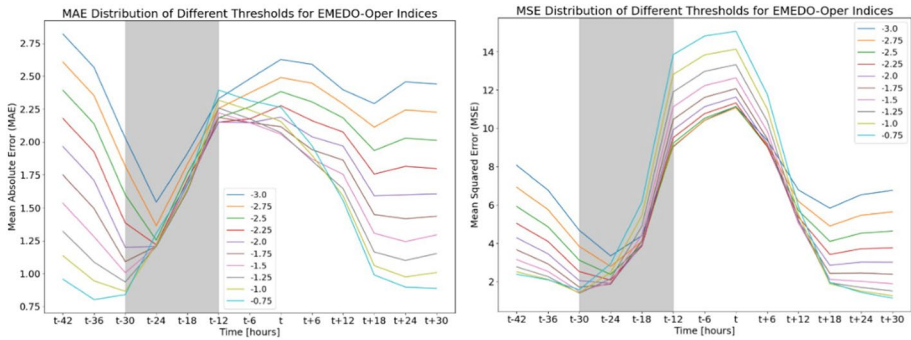


Fig. 19 Error distributions between the EMEDO-Oper indice values (the vertical axis) of -0.75 and -3.0 for time period (the horizontal axis) of 42 h before to 30 h after for selected tornado events. Mean Absolute Error (left) and Mean Square Error (right)

local minimum occurs, the two distinct time spans “t-42 to t-6” and “t-30 to t-12” in highly correlated events must indicate the probable occurrence period of the tornado.

In the tornado event of January 9 (Fig. 20), the EMEDO-Oper value declined to -0.6 around 12 h and 20 min before the tornado occurred, with other EMEDO variants exhibiting a similar trend. However, after the occurrence, the variations continued to oscillate in a highly distributed and irregular manner.

In the March 2 tornado incident (Fig. 21), all EMEDO variations are distributed in a balanced manner. The exception in this case is that it took a considerable amount of time for the local minimum value to be reached, that is, to exceed the value of -7 , and the index remained in the negative phase for a substantial amount of time until it reached the turning point. During this phase of negative growth, the EMEDO-Max variation and the EMEDO-3 variation followed distinct patterns.

On April 19th (Fig. 22), notably harmonious patterns appeared during the tornado. This is due to the fact that the ULL crosses directly above the EMEDO_i west polar region. A negative EMEDO phase was detected, which was significant in comparison with other occurrences.

The EMEDO value of the 15 October case is remarkably low (Fig. 23), but its development is extremely abrupt. The time required to move from the positive phase to the negative phase and attain the local minimum value is only 12 h. A second tornado was detected 12 h after the minimum for the region. EMEDO-Max and EMEDO-3 split themselves from other members and followed the same path.

According to the plot on November 7 (Fig. 24), the tornado that hit roughly 27 h after the local minimum happened in a condition where the EMEDO-Oper member was negative yet weak. Before all members reached the local minimum, there was a minor upward fluctuation in the EMEDO-2 member and a downward fluctuation in the EMEDO-Max member, but the EMEDO-Oper variation steadily collected strength in the negative phase for about 24 h and reached the local minimum mode. However, after the occurrence, the EMEDO-Oper variation remained in a slightly positive phase.

Prior to the tornado, it was noticed that the EMEDO index values had a falling trend in all events, as predicted, but after the tornado it rebounded to a neutral phase. Based on a prediction to be made at the local minimum, the formation of the tornado

Table 6 Performance statistics of accuracy metrics according to the EMEDO-Oper = -0.75 during the period of tornadic storm (including local minimum time and tornado time) for all events in Türkiye

Time	t-42	t-36	t-30	t-24	t-18	t-12	t-6	t	t+6	t+12	t+18	t+24	t+30
MAE	0.96	0.80	0.84	1.31	1.69	2.39	2.31	2.26	1.97	1.56	0.99	0.90	0.89
MBE	0.14	-0.08	-0.44	-1.03	-1.52	-2.20	-2.10	-2.00	-1.66	-0.93	-0.26	0.01	0.13
MPE	6.61	-3.66	3.05	3.37	1.14	0.10	-3.66	3.72	2.60	0.58	-6.28	20.80	8.96
MSE	2.38	2.09	1.58	2.93	6.17	13.85	14.82	15.08	11.79	5.92	1.95	1.43	1.14
MAPE	14.21	7.24	5.22	4.10	1.22	0.85	4.57	4.25	3.41	6.98	65.95	22.84	12.31
RMSE	1.54	1.45	1.26	1.71	2.48	3.72	3.85	3.88	3.43	2.43	1.40	1.20	1.07
RMSLE	-0.57	-0.49	-0.48	-0.62	-0.74	-0.89	-0.88	-0.86	-0.80	-0.72	-0.56	-0.53	-0.50

Values indicate mean bias error (MBE), mean absolute error (MAE), mean squared error (MSE), root mean square error (RMSE), root mean square logarithmic error (RMSLE), mean percentage error (MPE), and mean absolute percentage error (MAPE), which are statistically significant positive correlations at 95% confidence level

Table 7 Correlation statistics of cumulative minimum of EMEDO-Oper indices during the period of tornadoic storm (including local minimum time and tornado time) for all events in Türkiye

Time	CC		CD		CDadj	
	Pearson	Spearman	Pearson	Spearman	Pearson	Spearman
t-30–t-12	0.83	0.91	0.69	0.82	0.66	0.81
t-42–t-6	0.86	0.95	0.75	0.89	0.73	0.89

Values indicate correlation coefficient (CC), coefficient of determination (CD), adjusted version of coefficient of determination (CD_{adj}), which are statistically significant positive correlations at 95% confidence level

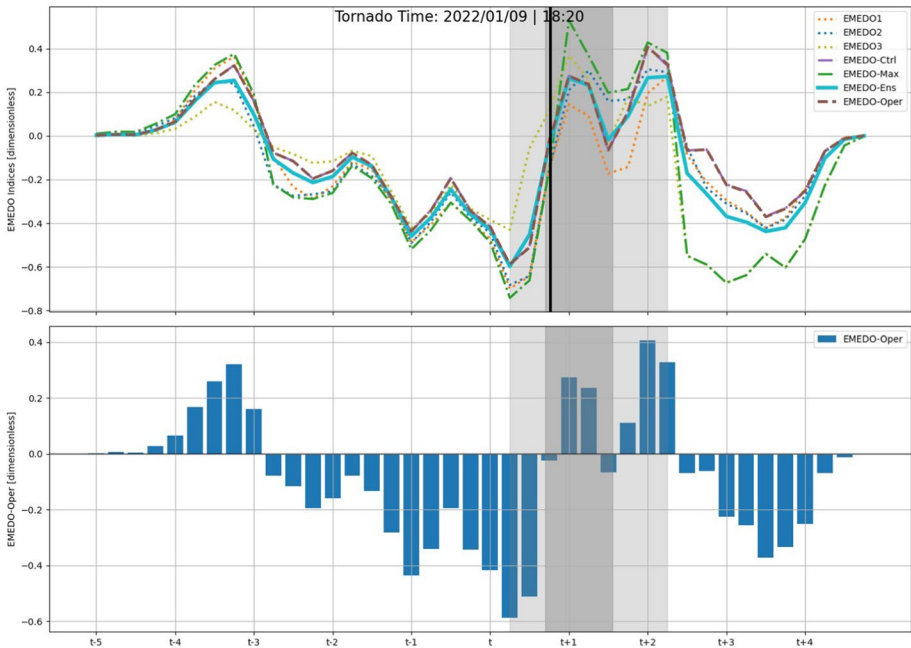


Fig. 20 During the 72 h preceding the tornado (the horizontal axis), all members of EMEDO_i (top) and EMEDO-Oper index (bottom) were analyzed for 09.01.2022 event of verification (the vertical axis) from Table 4. The lightly colored regions reflect the sixth to forty-second hours following the local minimum peak of the EMEDO- Oper index. The opaque inner regions indicate the 12th to 30th hours following the local minimum peak of the same index. The vertical black line depicts the instant the tornado occurred

is predicted to occur within the following 6–42 h, or as it approaches the neutral phase. Also, as previously discussed, although the -0.75 threshold value is statistically reliable with a minimum margin of error, it is not reliable for newly occurring case scenarios.

In light of this information, it appears that forecasts of tornado occurrence time intervals based on the EMEDO index would be consistent for all events when evaluated in terms of the relationship between a declining and an increasing trend, regardless of the magnitude of index value. The algorithm we have developed is not designed to specifically detect individual tornadoes. Instead, it provides a risk assessment, indicating the likelihood or potential of tornado occurrences in a given area. By analyzing broader atmospheric conditions

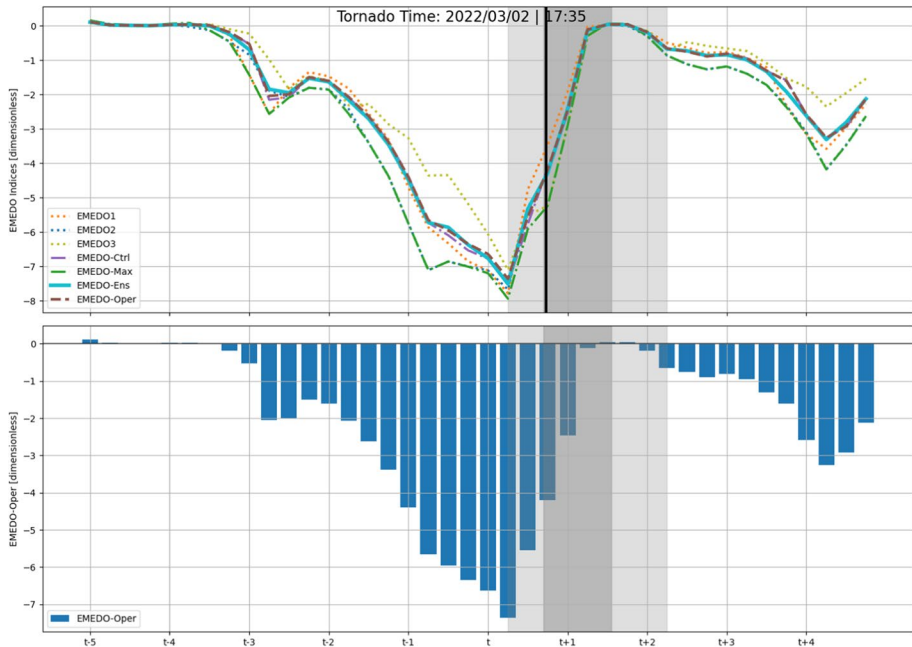


Fig. 21 During the 72 h preceding the tornado (the horizontal axis), all members of EMEDO $_i$ (top) and EMEDO-Oper index (bottom) were analyzed for 02.03.2022 event of verification (the vertical axis) from Table 4. The lightly colored regions reflect the sixth to forty-second hours following the local minimum peak of the EMEDO- Oper index. The opaque inner regions indicate the 12th to 30th hours following the local minimum peak of the same index. The vertical black line depicts the instant the tornado occurred

and patterns, the model offers advance warnings about regions with heightened tornado risks. It is essential to understand that the model's primary function is to aid in early preparedness and awareness, rather than pinpointing exact tornado locations.

7 Summary and concluding remarks

To reduce the impacts of severe convective storms and tornadoes in the scope of climate change adaptation strategies, Eastern Mediterranean oscillation index (EMEDO $_i$) has been developed in order to be able to detect the presence of ULLs and frontogenesis approach is employed for selected tornadic storm events in Türkiye. EMEDO $_i$ has 7 different its variations (members). These members have been developed to detect differences depending on the entry directions of cyclones and storms affecting Türkiye from the west of the country. In line with the GDAS data analysis, values of geopotential height are derived for the requirement of EMEDO $_i$ in a limited area.

In all the verification events, it is evident that tornadic SCS activities in Türkiye rise during the initial days when the EMEDO $_i$ transitions from a negative to a neutral phase. However, it is not clear that a stronger shift in this phase directly correlates with increased storm damage. The formation of a front over the Eastern Mediterranean is pivotal, and the way this front interacts with Türkiye's climate plays a significant © role in shaping the conditions conducive for these storms. Before the onset of tornado events, data indicates a

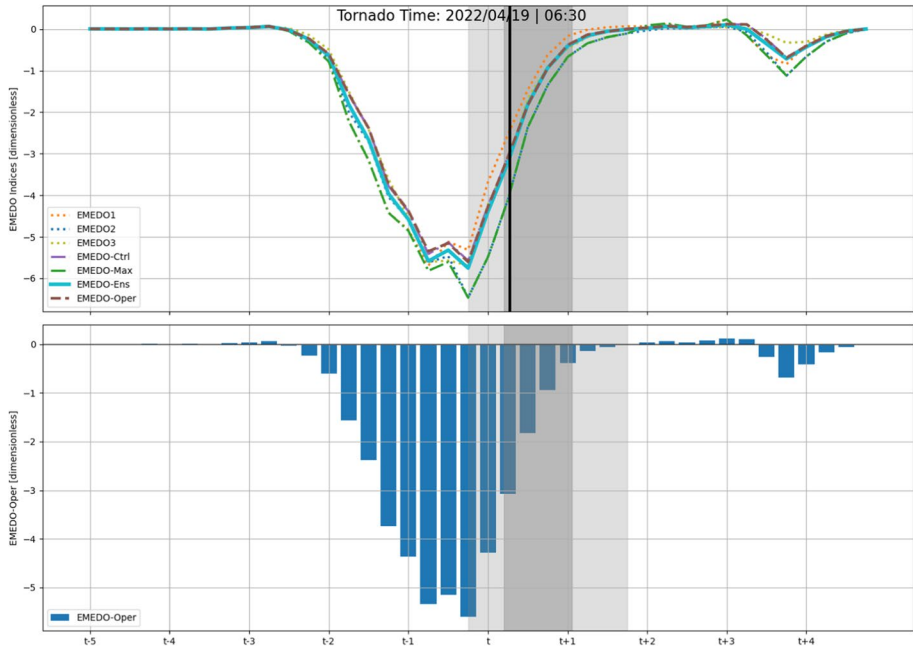


Fig. 22 During the 72 h preceding the tornado (the horizontal axis), all members of EMEDO_i (top) and EMEDO-Oper index (bottom) were analyzed for 19.04.2022 event of verification (the vertical axis) from Table 4. The lightly colored regions reflect the sixth to forty-second hours following the local minimum peak of the EMEDO-Oper index. The opaque inner regions indicate the 12th to 30th hours following the local minimum peak of the same index. The vertical black line depicts the instant the tornado occurred

decline in geopotential thickness difference values at points *P1–3* and *C*, which encompass regions like Italy, Greece, and Albania. Concurrently, there is a noticeable increase in the difference between isohypse values across the poles, attributed to the pronounced temperature gradient at 300 hPa.

As the spread of all members of EMEDO_i expanded with forecast time, it took on different values than EMEDO-Ens or EMEDO-Oper, making it more difficult to explain the consequences of modifying or determining non-mesocyclonic waterspouts and mesocyclonic supercell tornado structures. Consequently, it may also be claimed that the amplitude of the EMEDO perturbations may have been either small or too large for a severe weather warning, and that the EMEDO spatial variability (noisy patterns) may have diminished the signal.

The key results of the study are as follows:

- 86% of the events in the train list demonstrated that the EMEDO-Oper index was in negative phase at the time a tornado was reported, regardless of whether the events involved by a supercell mesoscale convective storm or a frontal movement. At the time of the tornado, the values of consisting of a small portion of the train cluster can only qualify as neutral phase. However, a turning point may take place at the local lowest point of the negative phase just before or around the hours that tornado events happen. This includes non-mesocyclonic waterspouts that are induced by the sea.

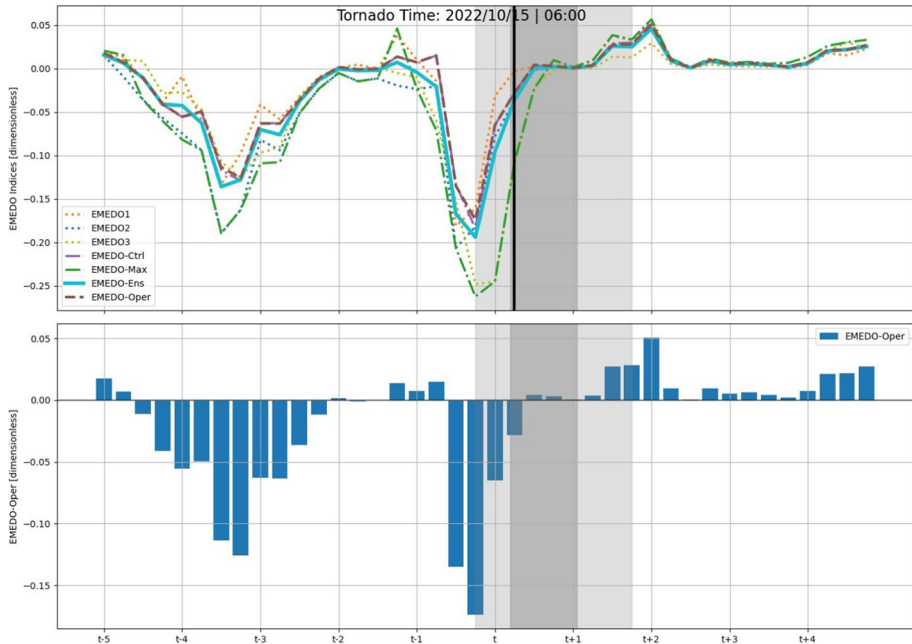


Fig. 23 During the 72 h preceding the tornado (the horizontal axis), all members of EMEDO_i (top) and EMEDO-Oper index (bottom) were analyzed for 15.10.2022 event of verification (the vertical axis) from Table 4. The lightly colored regions reflect the sixth to forty-second hours following the local minimum peak of the EMEDO-Oper index. The opaque inner regions indicate the 12th to 30th hours following the local minimum peak of the same index. The vertical black line depicts the instant the tornado occurred

- Each tornado incident in the western region of Türkiye occurred at a different time of day, but the daytime is more favorable.
- The EMEDO reflects the variations in atmospheric pressure in the Eastern Mediterranean. When it's strongly negative, it signals notable low-pressure areas within the defined triangle region. This creates a sharper difference between low and high-pressure regions, influencing their relative altitudes. Hence, the greater the negative EMEDO phase, the deeper the geopotential gradient between the trough over Italy, Greece, and Albania and the ridge in the vicinity of Israel; as a result, the environmental conditions in the Eastern Mediterranean are more favorable for the formation of a frontogenesis. Besides, the strength of fronts was generally observed as strong classification which is defined as more than 8 K per 110 km. In a few cases of events which are reported as waterspout, the strength of the fronts can be considered moderate classification (4 K/110 km).
- The amount of time needed to reach the local minimum perpetually varies depending on the event. This timescale is estimated to be 31.3 h on average based on the tornadic storm environment in the train cluster; however, when the tornado activity in 2022 is taken into account, this time frame is estimated to be 33.2 h instead.
- Between 6 and 42 h after the EMEDO-Oper index reaches its local minimum, a tornado can be expected with a 79% probability in western Türkiye. More specifically, the probability for this period is predicted to be 63% between 12 and 30 h after the

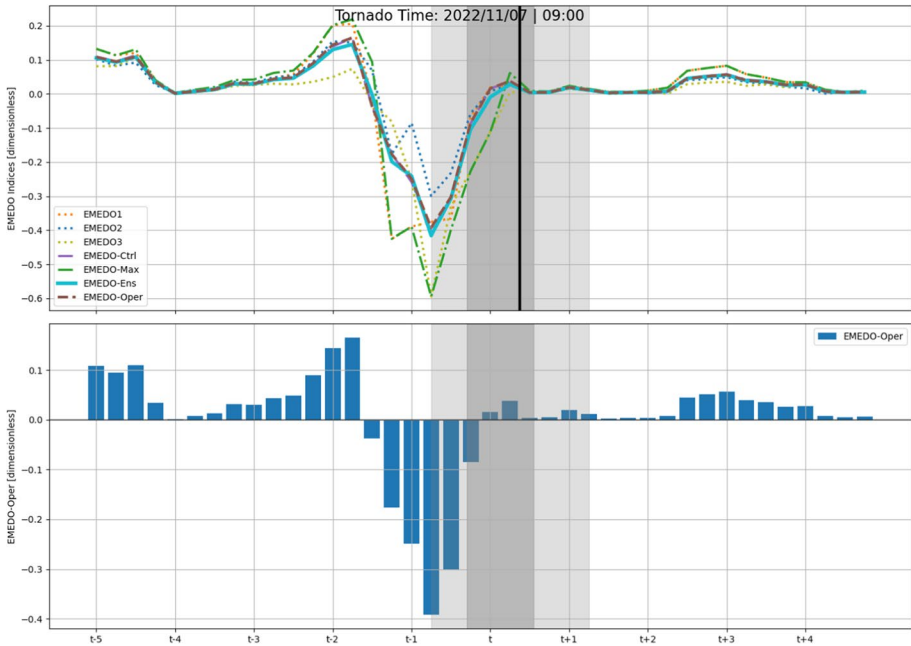


Fig. 24 During the 72 h preceding the tornado (the horizontal axis), all members of EMEDO_i (top) and EMEDO-Oper index (bottom) were analyzed for 07.11.2022 event of verification (the vertical axis) from Table 4. The lightly colored regions reflect the sixth to forty-second hours following the local minimum peak of the EMEDO-Oper index. The opaque inner regions indicate the 12th to 30th hours following the local minimum peak of the same index. The vertical black line depicts the instant the tornado occurred

local minimum has been determined. Once the local minimum has been reached, the remaining events typically occur within the next couple of hours.

- Based on the EMEDO-Oper values of the analyzed events, the majority of the events had index values below -0.75 . It is therefore possible to expect a risky period in Türkiye with a 79% probability after an EMEDO-Oper index value drops below -0.75 and the local minimum point needs to be determined.
- When local minimum values are reached, a tornado is likely to occur after the tendency to move to the neutral phase. For instance, as can be seen in the event of January 09, 2022, there were three local minimum attempts toward neutral phase. There have been reports of tornadoes in other provinces that were not included in the sample list in related dates.

Moreover, one of the challenges for the study was the temporal resolution of analysis data. Although interpolating analysis data seems like a solution, 1-h forecast data, which is preferred for ecologic models in operational use today, will be more useful to follow the EMEDO index.

Another limitation was that the narrow presence of photos of tornadic storms in media. Although the tornado events that have been analyzed are the ones that have taken place in the last years and have photographs, as much as possible, more photographs are needed to understand the structure of the tornado. It would be beneficial to determine whether they are mesocyclonic or not. This is because, although too many small and harmless

(non-mesocyclonic) waterspouts have been reported, the tornado events reported within the scope of this study are considered independent of mesocyclonic features. The reason for this is that the development process of each frontal or convective precipitation system should be examined through radar/satellite data tracking and whether the storm structure is mesocyclonic or not. Sometimes these meteorological systems intensify as they approach Türkiye and can take on a super-cellular structure. As stated in study's purpose of shedding light, the EMEDO index can be a guide; however, these systems should be analyzed by modeling them operationally with high resolution for the limited period determined by EMEDO.

The further research step would be using EMEDO_i to detect an ULL that is expected to influence Türkiye. According to the researches, it is argued that polar arctic or Icelandic cold strikes will affect Eastern Europe more frequently as a result of the widening of high-pressure belts around subtropics within the scope of climate change. According to the researches made by some articles, in parallel, the Azores high-pressure center gaining a more stable and vertically moving structure to become Arctic Ridge (AR) and BLO+ through the high latitudes in the north. This may make the indicators of EMEDO negative phases more frequent in the future. If it would be delved deeper into the subject by utilizing weather research and forecasting model (WRF), which is one of the prominent models on mesoscale numerical weather prediction, the major aspects of numerically simulating a tornado and its formation might be reviewed. In this way, the dynamics of tornado formation and structure based on both observations and laboratory and numerical weather prediction modeling experiments could be described in detail.

These storms contain secondary circulation and front inclination with the advection in the cold front transition should be thoroughly examined. In this way, it is possible to predict the convective trigger mechanisms and weather phases and ultimately have a forecasting approach for them. Besides, vertical layers should be resolved and elaborately modeled to obtain the features of thunderstorms such as storm motion speed/direction, critical angle, convection energy and relative winds. These opportunities contribute to geospatial point-based tornado forecasts however operating the model of high-resolution numerical weather prediction computational costs very huge amount for the institutes and national weather services. Consequently, there is a need to examine severe weather events in the Eastern Mediterranean region, including Türkiye and to reveal the clues that the events will take place a few days in advance. At this point, there is a necessity for a composite index showing that the Mediterranean atmospheric conditions expected to influence the Eastern will trigger the formation of severe convective storms.

Besides, a more convincing relationship analysis could be improved in the near future, using the point reporting of the tornado events and the probability of triggering negative EMEDO index. At this point, Brier scores can provide information about how accurate a forecast was because a brier score is a way to verify the accuracy of a probability forecast. A forecast probability can refer to a specific event, such as there is a 25% probability of it occurs a tornado in the next 24 h. In addition to that, Brier Skill Score also can be considered as a follow-up analysis. Although this index is not only considered within the scope of tornadic storms, but also it is estimated that it can be used for most extreme weather events (blizzards, hailstorms, wind damages, and so forth). In particular, institutions may have the opportunity to examine in more detail with the help of this index in terms of hailstorms, snowstorms or any other severe weather events affecting Türkiye all the year round.

To sum up, the study discussed how the ULL transport conditions into the Eastern Mediterranean are influenced in associated with lower and upper-level geopotential height changes over the Euro-Mediterranean sector. The findings may contribute to studies for

numerical weather prediction modeling in terms of low-level moisture, instability, lifting trigger mechanism and wind shear transport sensitivity into the Euro-Mediterranean, and its relationship with the tornadic storm activities over the Eastern Mediterranean region.

Author contributions All authors contributed to the study conception and design. Material preparation, data collection and analysis were performed by OKM, SAS and SK. The first draft of the manuscript was written by OKM and all authors commented on previous versions of the manuscript. All authors read and approved the final manuscript.

Funding Open Access funding enabled and organized by Projekt DEAL. The authors declare that no funds, grants, or other support were received during the preparation of this manuscript.

Declarations

Conflict of interest All authors certify that they have no affiliations with or involvement in any organization or entity with any financial interest or non-financial interest in the subject matter or materials discussed in this manuscript.

Open Access This article is licensed under a Creative Commons Attribution 4.0 International License, which permits use, sharing, adaptation, distribution and reproduction in any medium or format, as long as you give appropriate credit to the original author(s) and the source, provide a link to the Creative Commons licence, and indicate if changes were made. The images or other third party material in this article are included in the article's Creative Commons licence, unless indicated otherwise in a credit line to the material. If material is not included in the article's Creative Commons licence and your intended use is not permitted by statutory regulation or exceeds the permitted use, you will need to obtain permission directly from the copyright holder. To view a copy of this licence, visit <http://creativecommons.org/licenses/by/4.0/>.

References

- Bluestein HB (2013) Severe convective storms and tornadoes. Springer, 10:978–981
- Carvalho LM, Jones C, Liebmann B (2002) Extreme precipitation events in southeastern South America and large-scale convective patterns in the South Atlantic convergence zone. *J Clim* 15(17):2377–2394
- Cassou C (2008) Intraseasonal interaction between the Madden–Julian oscillation and the North Atlantic Oscillation. *Nature* 455(7212):523–527
- Cassou C (2010) Euro-Atlantic regimes and their teleconnections. In: Seminar on Predictability in the European and Atlantic regions from days to years, 6–9 September 2010, Shinfield Park, Reading. ECMWF, pp 6–9
- Criado-Aldeanueva F, Soto-Navarro J (2020) Climatic indices over the Mediterranean Sea: a review. *Appl Sci* 10(17):5790
- Diaz HF, Murnane RJ (2008) Climate extremes and society. Cambridge University Press
- Doswell CA (2001) Severe convective storms—an overview. In: Severe convective storms, pp 1–26
- Dotzek N, Groenemeijer P, Feuerstein B, et al (2009) Overview of ESSL's severe convective storms research using the European Severe Weather Database ESWD. *Atmos Res* 93:575–586. URL <https://www.essl.org/cms/severe-weather-season-2019-summary/>
- Durkee JD, Mote TL, Shepherd JM (2009) The contribution of mesoscale convective complexes to rainfall across subtropical South America. *J Clim* 22(17):4590–4605
- Grimm AM, Tedeschi RG (2009) ENSO and extreme rainfall events in South America. *J Clim* 22(7):1589–1609
- Haylock MR, Goodess CM (2004) Interannual variability of European extreme winter rainfall and links with mean large-scale circulation. *Int J Climatol J R Meteorol Soc* 24(6):759–776
- Kahraman A (2021) Synoptic climatology of supercell-type tornado and very large hail days in Türkiye. *Weather* 76:129–134
- Kahraman A, Markowski PM (2014) Tornado climatology of Türkiye. *Mon Weather Rev* 142(6):2345–2352
- Kahraman A, Kadioglu M, Markowski PM (2017) Severe convective storm environments in Türkiye. *Mon Weather Rev* 145(12):4711–4725

- Khandekar ML (2013) Are extreme weather events on the rise? *Energy Environ* 24(3–4):537–549. <https://doi.org/10.1260/0958-305X.24.3-4.537>
- Markowski P, Richardson Y (2011) *Mesoscale meteorology in midlatitudes*. Wiley
- Martin-Vide J, Lopez-Bustins JA (2006) The western Mediterranean oscillation and rainfall in the Iberian Peninsula. *Int J Climatol J R Meteorol Soc* 26(11):1455–1475
- Pučík T, Groenemeiger P, Tsonevsky I (2021) Vertical wind shear and convective storms. European Centre for Medium-Range Weather Forecasts
- Rasmussen EN, Blanchard DO (1998) A baseline climatology of sounding-derived supercell and tornado forecast parameters. *Weather Forecast* 13:1148–1164
- Sanders F (1999) A proposed method of surface map analysis. *Mon Weather Rev* 127(6):945–955
- Sirdas S, Sen Z (2003) Spatio-temporal drought analysis to the Trakya region. *Hydrol Sci J* 28:809–830
- Sirdas S, Sen Z, Oztopal A (2013) Climate change expectations in the next half century of turkey. Causes impacts and solutions to global warming. Springer, New York, pp 103–127. https://doi.org/10.1007/978-1-4614-7588-0_6
- Sirdas SA, Tuncay Özdemir E, Sezen İ et al (2017) Devastating extreme Mediterranean cyclone's impacts in Turkey. *Nat Hazards* 87:255–286. <https://doi.org/10.1007/s11069-017-2762-1>
- Türkeş M (1996) Spatial and temporal analysis of annual rainfall variations in Turkey. *Int J Climatol: J R Meteorol Soc* 16(9):1057–1076
- Vasconcellos FC, Cavalcanti IF (2010) Extreme precipitation over Southeastern Brazil in the austral summer and relations with the Southern Hemisphere annular mode. *Atmos Sci Lett* 11(1):21–26
- WMO (2021) Atlas of mortality and economic losses from weather, climate and water extremes (1970–2019) (WMO-No. 1267)

Publisher's Note Springer Nature remains neutral with regard to jurisdictional claims in published maps and institutional affiliations.

Authors and Affiliations

Omer Kutay Mihliardic¹  · Sevinc Asilhan Sirdas² · Serkan Kaya³

- ✉ Omer Kutay Mihliardic
mihliardic@meteo.uni-hannover.de
- ✉ Sevinc Asilhan Sirdas
sirdas@itu.edu.tr
- ✉ Serkan Kaya
serkan.kaya@student.kit.edu

¹ Institute of Meteorology and Climatology, Leibniz University Hannover, Herrenhäuser Str. 2, 30419 Hannover, Germany

² Department of Meteorological Engineering, Faculty of Aeronautics and Astronautics, Istanbul Technical University, 34469 Maslak, Istanbul, Turkey

³ Institute of Meteorology and Climate Research, Karlsruhe Institute of Technology, Wolfgang-Gaede-Strasse 1, 76131 Karlsruhe, Germany